

Algebraic Connectivity Maximization for Air Transportation Networks

Peng Wei, *Member, IEEE*, Gregoire Spiers, and Dengfeng Sun, *Member, IEEE*

Abstract—It is necessary to design a robust air transportation network. An experiment based on the real air transportation network is performed to show that algebraic connectivity is a fair measure for network robustness under random failures. Therefore, the goal of this paper is to maximize algebraic connectivity. Some researchers solve the maximization of the algebraic connectivity by choosing the weights for the edges in the graph. Others focus on the best way to add edges in a network in order to optimize the connectivity. In this paper, the authors formulate a new air transportation network model and show that the corresponding algebraic connectivity optimization problem is interesting because the two subproblems of adding edges and choosing edge weights cannot be treated separately. The new problem is formulated and exactly solved in a small air transportation network case. The authors also propose the approximation algorithm in order to achieve better efficiency. For large networks, the semidefinite programming with cluster decomposition is first presented. Moreover, the algebraic connectivity maximization for directed networks is discussed. Simulations are performed for a small-scale case, large-scale problem, and directed network problem.

Index Terms—Author, please supply index terms/keywords for your paper. To download the IEEE Taxonomy go to http://www.ieee.org/documents/Taxonomy_v101.pdf.

I. INTRODUCTION

AN AIR transportation network consists of distinct airports (cities) and direct flight routes between airport pairs [1]. Usually, a graph $G(V, E)$ is used to describe an air transportation network [2], [3], where the node set V represents all the n airports and the edge (link) set E represents all the m direct flight routes between airports. If a direct flight route from airport a to airport b exists, normally, the direct return route from airport b to airport a also exists [4]; $G(V, E)$ is constructed as an undirected simple graph, where the airports are indexed as $\{v_i | i = 1, 2, \dots, n\}$ and the direct flight routes are named as e_{ij} if there is a direct route between airports v_i and v_j . There are many factors to be considered when designing an air transportation network, such as traffic demand, operating cost, airport hubs, market competition, multiairport systems, and

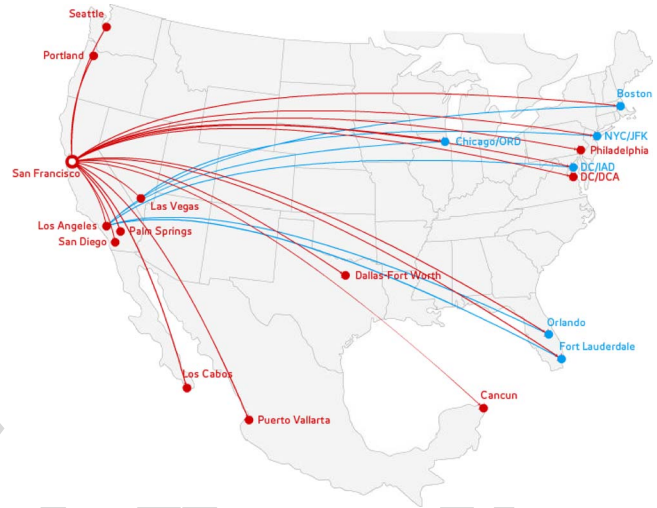


Fig. 1. Air transportation network route map for Virgin America Airlines.

scheduling [5]–[14]. In this paper, we focus on investigating the network robustness maximization, particularly the algebraic connectivity maximization.

A. Algebraic Connectivity and Air Transportation Network Robustness

In order to illustrate the relationship between the algebraic connectivity and air transportation network robustness, a real air transportation network of Virgin America is studied. The following experiment shows that algebraic connectivity is a fair measurement for the network robustness with regard to random link failures under the current Virgin America network topology.

According to the current route map of Virgin America in Fig. 1, we consider the 16 airports in the United States and obtain the adjacency matrix as Table I. The 16 United States airports include Boston (BOS), New York City/John F. Kennedy (JFK), Philadelphia, Washington Dulles International Airport (DC/IAD), Ronald Reagan Washington National Airport (DC/DCA), Chicago O’Hare International Airport (ORD), Orlando, Fort Lauderdale, Dallas/Fort Worth, Seattle, Portland, San Francisco, Los Angeles, Las Vegas, San Diego, and Palm Springs and are indexed as numbers 1–16. San Francisco International Airport (SFO) and Los Angeles International Airport (LAX) are two major hubs of the entire network. Both have at least one direct flight to almost all the other airports.

In order to show how well the algebraic connectivity can measure the robustness of an air transportation network, we

Manuscript received November 6, 2012; revised April 5, 2013 and August 20, 2013; accepted October 1, 2013. The Associate Editor for this paper was J.-P. B. Clarke.

P. Wei is with the Operations Research and Advanced Analytics, American Airlines, Fort Worth, TX 76155 USA (e-mail: peng.wei@aa.com).

G. Spiers was with the Department of Applied Mathematics, École Polytechnique, 91120 Palaiseau, France. He is now with Amadeus S.A.S., 06902 Sophia Antipolis, France (e-mail: gregoire.spiers@polytechnique.org).

D. Sun is with the School of Aeronautics and Astronautics, Purdue University, West Lafayette, IN 47907 USA (e-mail: dsun@purdue.edu).

Color versions of one or more of the figures in this paper are available online at <http://ieeexplore.ieee.org>.

Digital Object Identifier 10.1109/TITS.2013.2284913

TABLE I
ADJACENCY MATRIX CONSISTS OF 16 VIRGIN AMERICA AIRLINES AIRPORTS IN THE USA

	1	2	3	4	5	6	7	8	9	10	11	12	13	14	15	16
1	0	0	0	0	0	0	0	0	0	0	0	1	1	0	0	0
2	0	0	0	0	0	0	0	0	0	0	0	1	1	1	0	0
3	0	0	0	0	0	0	0	0	0	0	0	1	1	0	0	0
4	0	0	0	0	0	0	0	0	0	0	0	1	1	0	0	0
5	0	0	0	0	0	0	0	0	0	0	0	1	0	0	0	0
6	0	0	0	0	0	0	0	0	0	0	0	1	1	0	0	0
7	0	0	0	0	0	0	0	0	0	0	0	1	1	0	0	0
8	0	0	0	0	0	0	0	0	0	0	0	1	1	0	0	0
9	0	0	0	0	0	0	0	0	0	0	0	1	1	0	0	0
10	0	0	0	0	0	0	0	0	0	0	0	1	1	0	0	0
11	0	0	0	0	0	0	0	0	0	0	0	1	1	0	0	0
12	1	1	1	1	1	1	1	1	1	1	1	0	1	1	1	1
13	1	1	1	1	0	1	1	1	1	1	1	1	0	0	0	0
14	0	1	0	0	0	0	0	0	0	0	0	1	0	0	0	0
15	0	0	0	0	0	0	0	0	0	0	0	1	0	0	0	0
16	0	0	0	0	0	0	0	0	0	0	0	1	0	0	0	0

69 created six different *weighted air transportation networks* with
70 the same topology in Table I by randomly assigning one of
71 the three types of *link weights* to each route. Each link weight
72 is an indication of link strength. A larger weight represents a
73 stronger link and a smaller weight shows that the corresponding
74 link is easier to fail. There are many reasons for route failure,
75 such as weather disturbance, long ground delay program, long
76 airspace flow program (AFP), aircraft mechanical problem, and
77 upline flight delay/cancellation. The route failure rate statis-
78 tics are published by each origin–destination pair (route) and
79 different routes have different features [15]. For example, the
80 route failure rate between JFK and BOS during summer is
81 higher than that between SFO and LAX because of the crowded
82 northeastern airspace (AFP is more frequent) and more summer
83 thunderstorms. Another example is that a shorter route is easier
84 to fail than a longer transcontinental route because: 1) airlines
85 usually put larger aircraft on transcontinental route, and these
86 aircraft are more robust to weather disturbance and 2) airlines
87 are more likely to cancel shorter route flights because the flight
88 frequency on a shorter route is higher; therefor, the passengers
89 on the canceled flight are easier to protect (be reaccommodated
90 to later flights). In summary, each route has its own features
91 and thus in our model we consider that they have different
92 possibilities for failure.

93 The three types of link weights are mapped to different link
94 failure probabilities (see Table II). The link failure probability
95 range [%0, %5] is obtained from the historical flight cancellation
96 rate between September 15, 2012, and November 15, 2012 [15].
97 A network failure is defined as the existence of at least one
98 pair of nodes that cannot access each other through any one or
99 multiple links. For each one of the six weighted networks, 1000
100 trials are performed. In each trial, every link fails randomly

TABLE II
MAPPING BETWEEN LINK WEIGHTS AND LINK FAILURE PROBABILITIES

link weight w_{ij}	1	2	3
link failure probability	5%	3%	1%

TABLE III
NETWORK FAILURE NUMBERS WITH DIFFERENT ALGEBRAIC
CONNECTIVITY VALUES

algebraic connectivity	total failures in 10000 trials
1.0306	1113
1.7586	991
1.8661	763
1.9711	571
2.3128	423
2.7393	355

according to the failure probabilities listed in Table II. The total
101 number of network failures is counted in 1000 random trials.
102 The results are shown in Table III with algebraic connectivity
103 sorted in ascending order.
104

We can see that with higher algebraic connectivity, the
105 network is more robust and has fewer network failures. With
106 lower weighted algebraic connectivity, the network is easier to
107 break down. Therefor, algebraic connectivity is a fair robustness
108 measure for the air transportation network, and we need to find
109 the maximized algebraic connectivity.
110

The air traffic demand is expected to continue its rapid
111 growth in the future. The Federal Aviation Administration
112 estimated that the number of passengers is projected to increase
113 by an average of 3% every year until 2025 [16]. The expanding
114 traffic demand on the current air transportation networks of
115 different airlines will cause more and more flight cancellations
116 with the limited airport and airspace capacities. As a result,
117 more robust air transportation networks are desired to sustain
118

119 the increasing traffic demand for each airline and for the entire
120 National Airspace System (NAS). This is the major motivation
121 of this paper.

122 B. Related Work

123 An air transportation network and its robustness have been
124 studied over the last several years. Guimera and Amaral first
125 studied the scale-free graphical model of the air transportation
126 network [1]. Conway showed that it was better to describe
127 the national air transportation system or the commercial air
128 carrier transportation network as a system of systems [17].
129 Bonnefoy showed that the air transportation network was scale
130 free with aggregating multiple airport nodes into meganodes
131 [18]. Alexandrov defined that on-demand transportation net-
132 works would require robustness in system performance [19].
133 The robustness of an on-demand network would depend on the
134 tolerance of the network to variability in temporal and spatial
135 dynamics of weather, equipment, facility, crew positioning, etc.
136 Kotegawa *et al.* surveyed different metrics for air transportation
137 network robustness, including betweenness, degree, centrality,
138 connectivity, etc. [20]. They selected clustering coefficient and
139 eigenvector centrality as the network robustness metrics in
140 their machine learning approach. Bigdeli *et al.* compared alge-
141 braic connectivity, network criticality, average degree, average
142 node betweenness, and other metrics [21]. Jamakovic *et al.*
143 found that algebraic connectivity was an important metric in
144 the analysis of various robustness problems in several typical
145 network models [22], [23]. Byrne *et al.* showed that algebraic
146 connectivity was the efficient measure for the robustness of
147 both small and large networks [24]. Vargo *et al.* in [3] chose
148 algebraic connectivity as the robustness metric and built the
149 optimization problem solved by the edge swapping-based tabu
150 search algorithm.

151 In this paper, we measure the robustness of air transportation
152 network by computing the algebraic connectivity, which is
153 usually considered as one of the most reasonable and efficient
154 evaluation methods [24], [25]. Although the maximized value
155 of algebraic connectivity is abstract, the optimized air trans-
156 portation network structure and weighting assignment provide
157 us the applicable design.

158 There are some literature on algebraic connectivity maxi-
159 mization. The problems studied can be divided into two cat-
160 egories, namely, the edge addition problem and the variable
161 weights problem.

- 162 1) **Edge addition problem:** The goal is to add or remove a
163 given number of k edges on a graph in order to get the best
164 algebraic connectivity. The edges to be added or removed
165 are selected from a candidate set. The algorithms that
166 have been developed to solve the problem include tabu
167 search [25], greedy algorithms [25], [26], and rounded
168 semidefinite programming (SDP) [26].
- 169 2) **Variable weights problem:** The edges of the graph are
170 fixed and the goal is to determine the edge weights in
171 order to maximize the algebraic connectivity. This is
172 a convex optimization problem that is often solved by
173 using an SDP formulation [27]–[29] or a subgradient
174 algorithm [30].

C. Contribution

175

The major contribution of this paper compared with what
176 has been studied is that we find that, in order to maximize
177 the algebraic connectivity, the edge addition problem and the
178 variable weights problem cannot be studied separately. Solving
179 one of them independently will only result in a suboptimal
180 solution. Therefore, we propose a new algorithm to solve both
181 problems at the same time. How to choose the edges of the
182 graph is demonstrated, as well as how to assign their weights.
183 In addition, we are the first to present the cluster decomposition
184 method to achieve better computation efficiency for large-scale
185 networks. We are also the first to discuss the algebraic connec-
186 tivity maximization for directed air transportation networks. 187

The rest of this paper is structured as follows. Section II
188 shows why this problem naturally arises in air transportation
189 networks and how it can be formulated. In Section III, the
190 problem is exactly solved for small networks, and the fact that
191 the two problems are not independent is highlighted. Then, the
192 authors present the SDP formulation and the more efficient full
193 algorithm, which includes relaxed SDP, and solution rounding
194 is proposed. In Section IV, the problem for large networks
195 is solved, the computational efficiency is analyzed, and the
196 numerical results are provided. The algebraic connectivity op-
197 timization for directed air transportation networks is presented
198 in Section V. Section VI concludes this paper. 199

II. PROBLEM FORMULATION

200

A graph G with n nodes and m edges is used to define an air
201 transportation network. Let $A = (a_{ij})$ be the adjacency matrix
202 of G . The Laplacian matrix $L = (l_{ij})$ of G is defined by 203

$$\begin{cases} l_{ij} = -a_{ij}, & \text{if } i \neq j \\ l_{ii} = \sum_{j=1}^n a_{ij}. \end{cases}$$

The eigenvalues of L are sorted $\lambda_1 \leq \lambda_2 \leq \dots \leq \lambda_n$. L is a 204
semidefinite positive matrix; thus, for all i , $\lambda_i \geq 0$. It is also
205 known that $\lambda_1 = 0$ since $Le = 0$ with $e = (1, \dots, 1)$ [31]. 206

Definition: The second smallest eigenvalue $\lambda_2(L)$ is the 207
algebraic connectivity of G . 208

Now, recall the two key properties of the algebraic connec- 209
tivity that will be used in this paper. 210

Property 1: Let $e = (1, \dots, 1) \in \mathbb{R}^n$ and 211

$$\Omega = \{x \in \mathbb{R}^n \mid \|x\| = 1, \quad e^T x = 0\}.$$

The Courant–Fischer principle [32] states that 212

$$\lambda_2 = \min_{x \in \Omega} x^T L x. \quad (1)$$

Property 2: Function $w \rightarrow \lambda_2(w)$ is concave with w denot- 213
ing the edge weight vector. This can be proven by seeing that
214 $\lambda_2(w)$ is the pointwise infimum of a family of linear functions
215 of w (see [27]) 216

$$\lambda_2(w) = \inf_{\|v\|=1, e^T v=0} v^T L v,$$

$$\lambda_2(w) = \inf_{\|v\|=1, e^T v=0} \sum_{(i,j) \in E} w_{ij} (v_i - v_j)^2.$$

217 The goal of this paper is to maximize the algebraic connec-
218 tivity of the network under several constraints.

219 There are $m = (n(n-1))/2$ edges in the complete sym-
220 metric graph. Each has a weight w_{ij} representing the link
221 strength, as described in Section I. The following constraints
222 are considered.

223 The edge weight representing link strength must be within
224 the range between the lower bound α and the upper bound β

$$\forall (i, j) \in E, \quad \alpha \leq w_{ij} \leq \beta.$$

225 When there is no edge connecting v_i and v_j , the corresponding
226 $w_{ij} = 0$.

227 There exists an operating cost c_{ij} for each link. In a real air
228 transportation network, the cost for a route contains the fuel
229 cost, aircraft maintenance cost, crew/flight attendant labor cost,
230 cost for arrival/departure slots at runways, cost for gates at
231 origin/destination airports, and cost for flying through airspace
232 (international flights). In this paper, we use one link cost to
233 represent the integrated operating cost. The operating cost is
234 higher for a stronger link for several practical reasons. For
235 example, we know that the most effective way to avoid a
236 mechanical problem cancelation is to have spare parts or even
237 a spare aircraft. Similarly, the most effective way to avoid a
238 cancelation caused by crew legality or crew scheduling is to
239 have enough standby crew. Both approaches can increase link
240 strength; at the same time, they introduce higher costs. As for
241 weather disturbances, to load extra fuel will give an aircraft
242 more flight plan options with which it can be rerouted to avoid
243 weather problems and prevent the cancelation. However, extra
244 fuel also introduces higher cost. In addition, larger aircraft are
245 more robust to weather disturbances. Nevertheless, to operate
246 a larger aircraft costs more because of more fuel needed, more
247 flight attendants, and even more crew (for international flights).
248 Therefore, in this paper, we consider the linear cost for link
249 strength. The total operating cost budget for all the links is
250 limited by

$$\sum_{ij} w_{ij} c_{ij} \leq C.$$

251 In summary, the complete problem that the authors aim at
252 solving is

$$\max_w \lambda_2(L(w)) \quad \text{s.t.} \quad \begin{cases} \sum_{ij} w_{ij} c_{ij} \leq C \\ w_{ij} \in \{0, [\alpha, \beta]\} \end{cases} \quad (\text{P})$$

253 A. Alternative Formulation

254 In order to be able to solve the problem, the authors need to
255 reformulate it by adding decision variables. The idea is to add,
256 for each edge (i, j) , a binary variable x_{ij} stating if there exists
257 an edge between v_i and v_j

$$x_{ij} = 1 \Leftrightarrow w_{ij} \neq 0.$$

258 This is useful since now the domain of w can be expressed as

$$\forall (i, j), \quad \alpha x_{ij} \leq w_{ij} \leq \beta x_{ij}.$$

The problem now becomes

259

$$\max_{x, w} \lambda_2(L(w)) \quad \text{s.t.} \quad \begin{cases} x_{ij} \in \{0, 1\} \\ \sum_{ij} w_{ij} c_{ij} \leq C \\ \alpha x_{ij} \leq w_{ij} \leq \beta x_{ij} \end{cases}$$

Then, variable k is added, which determines the number of 260
edges in the graph. The final formulation of the problem is 261

$$\max_{x, w, k} \lambda_2(L(w)) \quad \text{s.t.} \quad \begin{cases} \sum_{i,j} x_{ij} = k \\ x_{ij} \in \{0, 1\} \\ \sum_{i,j} w_{ij} c_{ij} \leq C \\ \alpha x_{ij} \leq w_{ij} \leq \beta x_{ij} \end{cases} \quad (2)$$

B. Difficulty

262

An important remark is that the problem cannot really be 263
split into two steps of first deciding whether $w = 0$ or not and 264
followed by choosing the appropriate weights. This is due to 265
the fact that there are lower bound and upper bound constraints 266
on w . However, assuming that the two steps are independent, a 267
decoupled approach can be tried first. The first step is to choose 268
edges for the empty graph that corresponds to the edge addition 269
problem introduced in [25] 270

$$\begin{aligned} & \max_x \lambda_2(L(x)) \\ & \text{s.t.} : \sum_i x_i = k, \quad x_i \in \{0, 1\}, \quad \sum_i x_i c_i \leq \frac{C}{\alpha} \end{aligned}$$

and the second step is to choose the weights on them 271

$$\begin{aligned} & \max_w \lambda_2(L(w)) \\ & \text{s.t.} : \sum_i w_i c_i \leq C, \quad \alpha y_i \leq w_i \leq \beta y_i, \quad y = x_{\text{opt}}. \end{aligned}$$

Later, it will be seen that, if this approach is used, the result will 272
not be optimal. 273

C. Relaxation

274

The relaxation (R) of the problem is obtained by allowing 275
noninteger values for x 276

$$\forall (i, j) \in E, \quad x_{ij} \in [0, 1].$$

This is the same as choosing $w \in [0, \beta]$ without variables x 277
and k . However, these variables will be necessary in order to 278
be able to get the integer solution from this relaxed one. It is 279
noticed that the solution of (R) is a concave function of k . 280

D. Concavity in k

281

The first important property is that the solution of (R) is 282
concave in k , which will be used in the golden section search 283
algorithm in Algorithm 1. More precisely, Λ is defined such that 284

$$\Lambda(k) = \max_{x, w} \lambda_2(L(w)) \quad \text{s.t.} \quad \begin{cases} \sum_i x_i = k \\ x_i \in [0, 1] \\ \sum_i w_i c_i \leq C \\ \alpha x_i \leq w_i \leq \beta x_i \end{cases}$$

285 *Property 3:* $\Lambda(k)$ is a concave function.

286 This property is important since it shows that the maximiza-
287 tion of the algebraic connectivity is related to the number of
288 edges in the graph. By solving the problem for very few values
289 of k , a good knowledge on k_{opt} can be obtained.

290 *Proof:* Consider k_1 and k_2 in \mathbb{R} and $\gamma \in [0, 1]$ such that
291 $\Lambda(k_i) > 0$ for $i = 1, 2$. The idea is to use the fact that $w \rightarrow$
292 $\lambda_2(L(w))$ is concave (please see Property 2).

$$\begin{aligned} & \Lambda(\gamma k_1 + (1-\gamma)k_2) \\ &= \max_{x,w} \lambda_2 \quad \text{s.t.} \quad \begin{cases} \sum_i x_i = \gamma k_1 + (1-\gamma)k_2 \\ x_i \in [0, 1] \\ \sum_i w_i c_i \leq C \\ \alpha x_i \leq w_i \leq \beta x_i \end{cases} \\ &\geq \max_{x,w} \lambda_2 \quad \text{s.t.} \quad \begin{cases} \sum_i x_i^{(1)} = k_1, & \sum_i x_i^{(2)} = k_2 \\ x_i^{(j)} \in [0, 1], & j = 1, 2 \\ x = \gamma x^{(1)} + (1-\gamma)x^{(2)} \\ \sum_i w_i c_i \leq C \\ \alpha x_i \leq w_i \leq \beta x_i \end{cases} \\ &\geq \max_{x,w} \lambda_2 \quad \text{s.t.} \quad \begin{cases} \sum_i x_i^{(1)} = k_1, & \sum_i x_i^{(2)} = k_2 \\ x_i^{(j)} \in [0, 1], & j = 1, 2 \\ w = \gamma w^{(1)} + (1-\gamma)w^{(2)} \\ \sum_i w_i c_i \leq C \\ \alpha x_i^{(j)} \leq w_i^{(j)} \leq \beta x_i^{(j)} \end{cases} \\ &\geq \gamma \max_{x,w} \lambda_2 \quad \text{s.t.} \quad \begin{cases} \sum_i x_i = k_1 \\ x_i \in [0, 1] \\ \sum_i w_i c_i \leq C \\ \alpha x_i \leq w_i \leq \beta x_i \end{cases} \\ &\quad + (1-\gamma) \max_{x,w} \lambda_2 \quad \text{s.t.} \quad \begin{cases} \sum_i x_i = k_2 \\ x_i \in [0, 1] \\ \sum_i w_i c_i \leq C \\ \alpha x_i \leq w_i \leq \beta x_i \end{cases} \\ &\geq \gamma \Lambda(k_1) + (1-\gamma)\Lambda(k_2) \end{aligned}$$

293 which proves that Λ is concave in k . ■

294 III. SMALL-SCALE AIR TRANSPORTATION NETWORKS

295 A. Exact Solution for Small Networks

296 If all weights have to be chosen within an interval, the
297 problem becomes a convex optimization problem and it can
298 be solved using an SDP solver. The idea here is to try all the
299 possible configurations for which all the weights are either 0
300 or in $[\alpha, \beta]$. Then, each configuration can be independently
301 optimized and the one that leads to the best result can be found.

302 Consider that n nodes are chosen randomly. There are $m =$
303 $(n(n-1))/2$ edges and 2^m configurations to test. For each
304 configuration, if Y is the set of the edges that are actually in
305 the graph, the following problem needs to be solved:

$$\max_w \lambda_2(L(w)) \quad \text{s.t.} \quad \begin{cases} \sum_{i,j} w_{ij} c_{ij} \leq C \\ \alpha \leq w_{ij} \leq \beta, & \forall (i,j) \in Y \\ w_{ij} = 0, & \forall (i,j) \notin Y. \end{cases}$$

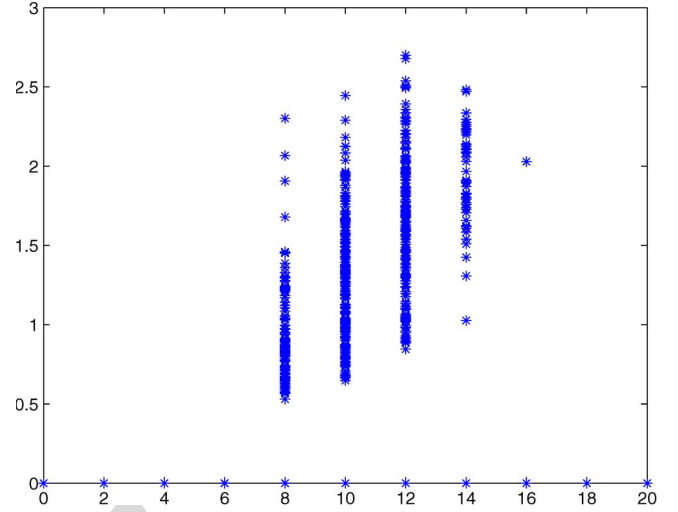


Fig. 2. Results of (k, λ_2) for all the configurations of $n = 5$ and $C = 6.5$.

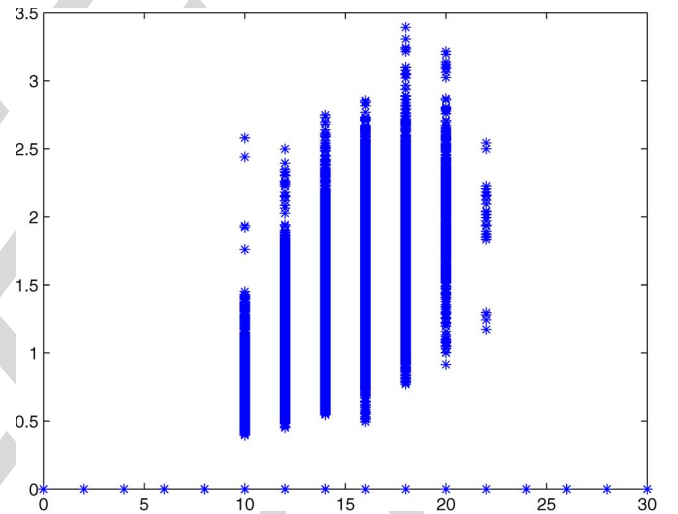


Fig. 3. Results of (k, λ_2) for all the configurations of $n = 6$ and $C = 8$.

This can be done by solving the SDP corresponding to the 306
weight optimization problem (see [27] for details) 307

$$\min_w \sum_i w_i c_i \quad \text{s.t.} \quad \begin{cases} \alpha \leq w_{ij} \leq \beta, & \forall (i,j) \in Y \\ w_{ij} = 0, & \forall (i,j) \notin Y \\ L(w) \succeq I - \frac{1}{n} ee^T. \end{cases}$$

It becomes impossible to exactly solve the problem when n is 308
large. Therefore, the authors assume n to be small in this section. 309

310 *1) Small-Scale Exact Solution Results:* For each configura-
311 tion, the number of edges k in the graph is computed. The
312 results of (k, λ_2) are plotted in Figs. 2 and 3 for two different
313 networks.

314 It is noticed that the best connectivity is not reached at the
315 maximum number of edges; therefore, the choice of the edges
316 and the choice of the weights are not independent. 316

317 It is also noticed that, unlike the continuous case, the discrete
318 shape given by $k \rightarrow \Lambda(k)$ in Figs. 2 and 3 is not exactly con-
319 cave. However, it has almost the shape of a concave function;
320 hence, the authors will be able to consider it concave in the
321 approximate case later on. 321

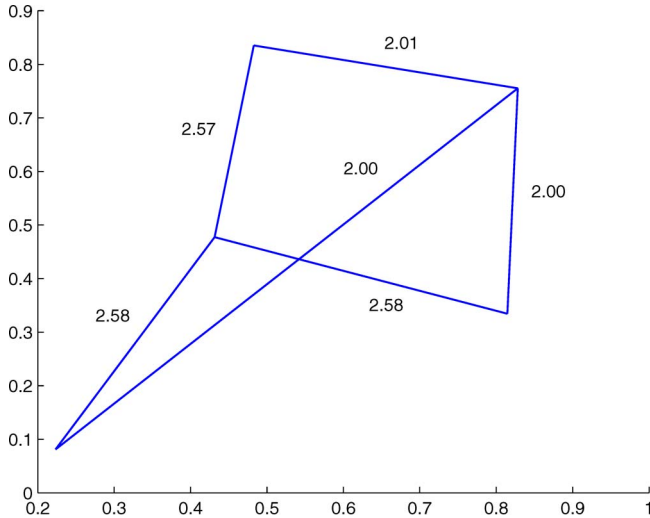


Fig. 4. Optimal network for $n = 5$ with the weights. $p = 0$, $\alpha = 2$, and $C = 6.5$.

322 The exact solution for a network of size $n = 5$ is shown
 323 in Fig. 4. As it is impossible to exactly solve this problem
 324 for networks with a larger size, an algorithm is going to be
 325 designed, which solves it approximately. The main idea is to
 326 use the quasi-concave shape of function $\Lambda(k)$.

327 For the practical problem with a larger size, the first step is to
 328 choose a value for k . The authors are able to solve the relaxed
 329 version (R) of the problem where x is a noninteger variable.
 330 Then, the result can be rounded to obtain a feasible solution for
 331 the original problem (P).

332 2) *Maximum Number of Edges*: Because of the minimum
 333 value α for the weights, there exists a limit in the number
 334 of edges in the graph. Here, the maximal number of edges
 335 k_{lim} needs to be found. Regardless of the performance of the
 336 network, edges are added until the operating cost constraint is
 337 reached. Consider that $w = \alpha x$, which is the minimum weight,
 338 and the problem is to solve a trivial form of the knapsack
 339 problem

$$\begin{aligned} & \max_{x \in \{0,1\}} \sum_i x_i \\ & \text{s.t. } \sum_i x_i c_i \leq \frac{C}{\alpha}. \end{aligned}$$

340 Indeed, if k_{lim} is the solution of this problem, it can be guaran-
 341 teed that there will not be any solution of $k > k_{\text{lim}}$.

342 When the cost c_i is sorted by increasing order, it can be
 343 obtained that

$$\sum_{s=1}^{k_{\text{lim}}} c_s \approx \frac{C}{\alpha}$$

344 which, for large-enough n , can be approximated by the follow-
 345 ing formula:

$$\int_1^{k_{\text{lim}}} g(s) ds = \frac{C}{\alpha}$$

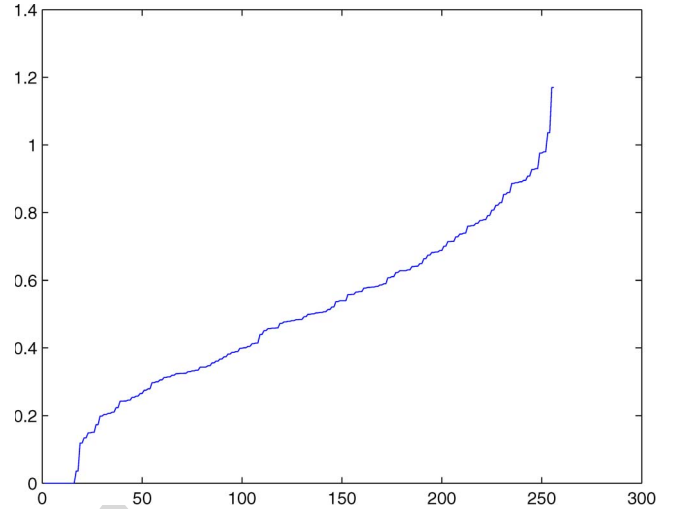


Fig. 5. Function g for random points in $[0, 1]^2$.

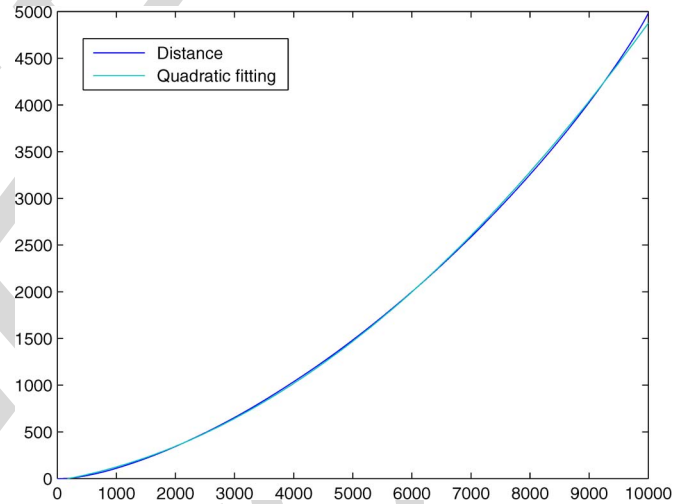


Fig. 6. C as a function of k_{lim} with the quadratic fitting.

where

$$\forall s \in [1, k_{\text{lim}}], \quad g(s) = c_{[s]}.$$

If the n nodes are randomly chosen in a square, function g 347
 is very close to a linear function (except at the very beginning 348
 and at the very end). This can be verified in Fig. 5. Using this 349
 information, it can be obtained that 350

$$a_2 k_{\text{lim}}^2 + a_1 k_{\text{lim}} + a_0 = \frac{C}{\alpha} \quad (3)$$

where a_0 , a_1 , and a_2 are constant parameters. Finally 351

$$k_{\text{lim}} = \frac{-a_1 + \sqrt{a_1^2 - 4a_2 \left(a_0 - \frac{C}{\alpha}\right)}}{2a_2}. \quad (4)$$

It is shown in Fig. 6 that the quadratic result obtained by (4) 352
 is a very good approximation. 353

354 *B. SDP Formulation*

355 To solve the larger size problem, the relaxation of the prob-
 356 lem is expressed as an SDP that will be solved efficiently. When
 357 v is not normalized, recall (1) in Property 1, which can be then
 358 transformed as

$$\begin{cases} \lambda_2 = \max_{\lambda} \lambda \\ \lambda v^T v \leq v^T L v \\ \forall v \in \mathbb{R}^n, \quad v^T e = 0. \end{cases}$$

359 Variable μ is added, which allows any $v \in \mathbb{R}^n$

$$\begin{cases} \lambda_2 = \max_{\lambda, \mu} \lambda \\ \forall v \in \mathbb{R}^n, \quad v^T (\mu e e^T) v + v^T L v - \lambda v^T v \geq 0. \end{cases}$$

360 It can be written using Loewner's order [33]

$$\begin{cases} \lambda_2 = \max_{\lambda, \mu} \lambda \\ \mu e e^T + L - \lambda I \succeq 0. \end{cases} \quad (5)$$

361 The relaxation of the problem that needs to be solved is

$$\max_{x, w, k} \lambda_2(L(w)) \quad \text{s.t.} \quad \begin{cases} \sum_i x_i = k \\ x_i \in [0, 1] \\ \sum_i w_i c_i \leq C \\ \alpha x_i \leq w_i \leq \beta x_i \end{cases}$$

362 which now becomes with (5)

$$\max_{x, w, k, \lambda, \mu} \lambda \quad \text{s.t.} \quad \begin{cases} \sum_i x_i = k \\ x_i \in [0, 1] \\ \sum_i w_i c_i \leq C \\ \alpha x_i \leq w_i \leq \beta x_i \\ \mu e e^T + L - \lambda I \succeq 0. \end{cases} \quad (6)$$

363 This problem is an SDP since there is a semidefinite constraint
 364 and all the other constraints are linear. It can be solved effi-
 365 ciently by an SDP solver. SeDuMi [34] is used in this paper.

366 1) *Optimality Conditions:* The primal SDP is

$$\max_{x, w, k, \lambda, \mu} \lambda \quad \text{s.t.} \quad \begin{cases} \sum_i x_i = k \\ x_i \in [0, 1] \\ \sum_i w_i c_i \leq C \\ \alpha x_i \leq w_i \leq \beta x_i \\ \mu e e^T + L - \lambda I \succeq 0. \end{cases}$$

367 The variables are rescaled by dividing w , k , and x by λ and C .

368 The dual SDP problem is

$$\min_{x, w, k, \lambda} \sum_i w_i c_i \quad \text{s.t.} \quad \begin{cases} \sum_i x_i = k \\ x_i \in [0, 1] \\ \alpha x_i \leq w_i \leq \beta x_i \\ L \succeq I - \frac{1}{n} J \end{cases}$$

369 where J is the all-one matrix. When x_{ij} is relaxed (please see
 370 Section II-C), the relaxed dual SDP formulation is

$$\min_{x, w, k, \lambda} \sum_i w_i c_i \quad \text{s.t.} \quad \begin{cases} 0 \leq w_i \leq \beta \\ L \succeq I - \frac{1}{n} J. \end{cases}$$

371 X is the matrix of the operating costs. The matrix format
 372 relaxed dual SDP is therefor

$$\max_X \left\langle I - \frac{1}{n} J, X \right\rangle \quad \text{s.t.} \quad \begin{cases} X \succeq 0 \\ \langle E, X \rangle = c_{ij} \end{cases}$$

373 where E is the matrix with $E_{ii} = E_{jj} = 1$ and $E_{ij} = E_{ji} = -1$.

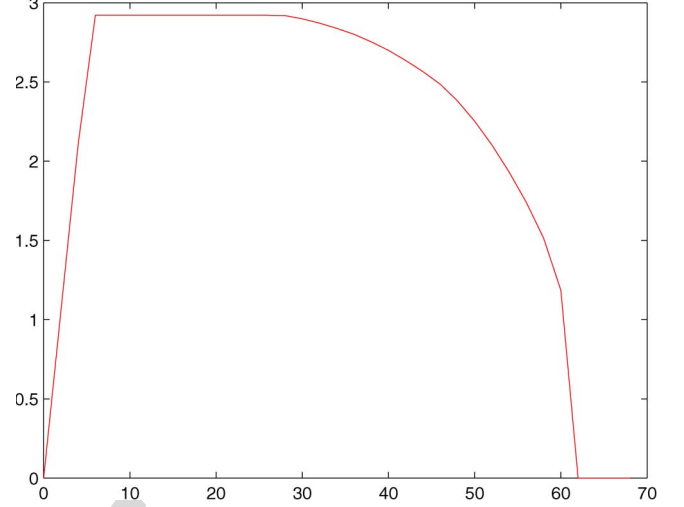


Fig. 7. Upper bound: $\lambda_2 = f(k)$.

The Karush–Kuhn–Tucker optimality conditions are

$$\begin{cases} SX = XS = 0 \\ S \succeq 0, \\ \langle E, X \rangle = c_{ij} \\ L - I + \frac{1}{n} J = S. \end{cases} \quad X \succeq 0$$

If $w_i = w$ for all i , it can be obtained that

$$S = (nw - 1) \left(I - \frac{1}{n} J \right).$$

When $w = 1/n$, $S = 0$ and the conditions are satisfied.

376 Reciprocally, if the optimality conditions are satisfied, it can
 377 be obtained that

$$\left(L - \left(I - \frac{1}{n} J \right) \right) X = 0.$$

X has rank n ; hence

$$L = I - \frac{1}{n} J.$$

Thus, w is constant for all i and $w = 1/n$.

381 For edge i and edge j , the optimality condition is finally
 382 obtained

$$\begin{cases} \forall(i, j), w_i = w_j \\ \sum_i w_i c_i = C. \end{cases}$$

2) *Upper Bound:* With the SDP formulation, the relaxation
 383 can now be solved. When the values of the optimal connectivity
 384 for different values of k are computed, the upper bound is
 385 plotted in Fig. 7.

386 The relaxed problem reached its maximum for several values
 387 of k contained in an interval $[k_{\min}, k_{\max}]$. Indeed, the optimal-
 388 ity conditions give

$$\begin{cases} \forall(i, j), w_i = w_j \\ \sum_{i=1}^m w_i c_i = C. \end{cases}$$

389 All the weights are equal and their value is $\forall i, w_i =$
 390 $(C / (\sum_j c_j)) = \Omega$. If $w = \beta x$, all the elements of x are equal

392 and their value is $\forall i, x_i = (k/(n^2 - n))$, which leads to

$$k_{\min} = \frac{\Omega(n^2 - n)}{\beta}.$$

393 By doing the same computation, it is proved that the optimal
394 value is also reached with

$$k_{\max} = \frac{\Omega(n^2 - n)}{\alpha}$$

395 and $\forall k \in [k_{\min}, k_{\max}]$, the optimal value is achieved.

396 However, it needs to be pointed out that when the solution
397 is rounded, infeasible solution may appear. For example, if $k =$
398 k_{\min} , there is often no solution since

$$\sum_i x_i = \frac{n\Omega}{\beta} < n - 1$$

399 if $(\Omega/\beta) \ll 1$, which is often the case. In addition, because at
400 least $n - 1$ edges are needed to connect an n node graph, there
401 is no positive solution. Therefore, the upper bound is not a very
402 good bound for small values of k .

403 C. Rounding Techniques for SDP Solution

404 1) *Description of the Methods:* In this section, suppose that
405 the relaxed optimal solution s_0 has been found. k edges are
406 going to be selected from s_0 , which means that $x_i = 1$ for k
407 values and $x_i = 0$ for the others. There are several ways to do
408 so. The methods that have been studied and implemented are
409 listed.

- 410 1) *Greedy:* Choose the k biggest elements $s_0(x_i)$ in the re-
411 laxed solution. Then, find the optimal weights by solving
412 the corresponding SDP.
- 413 2) *Random fast:* Randomly choose the rounding. For each
414 $i \in \{1, \dots, m\}$, $x_i = 1$ with probability $s_0(x_i)$ and $x_i =$
415 0 otherwise. Then, the weights are affected with the
416 following value:

$$\frac{s_0(w_i)}{s_0(x_i)}.$$

417 These two steps are repeated many times. The average
418 value $\overline{x_i}$ of x_i is $s_0(x_i)$; therefore

$$\overline{\sum_i x_i} = \sum_i s_0(x_i) = k$$

419 and for the same reason

$$\overline{\sum_i w_i c_i} = \sum_i \frac{s_0(w_i)}{s_0(x_i)} \overline{x_i} c_i = \sum_i s_0(w_i) c_i \leq C.$$

420 Thus, on average, the solution satisfies the constraints.
421 At the end, keep the best solution that satisfies all the
422 constraints.

- 423 3) *Random:* In addition, randomly choose the rounding. If
424 $\sum_i x_i = k$, which is the case on average, evaluate the
425 weights by solving the SDP formulation. The steps are
426 repeated several times, and keep the best value.

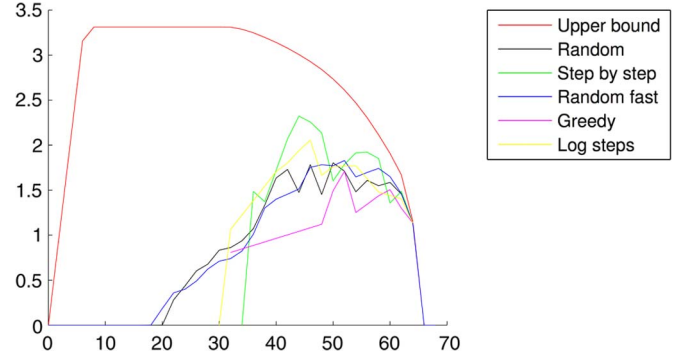


Fig. 8. λ_2 as a function of k . The results from several rounding methods are represented for a 20-node graph.

- 4) *Step by step:* Select the biggest element $s_0(x_i) < 1$ and
427 affect its value to 1 in the SDP formulation. Then, solve
428 the SDP again and repeat k times for these two steps. 429
- 5) *Log step by step:* This is the same idea as the “step by
430 step” except that, at each step, choose the best half of
431 the remaining elements. Thus, there are only $\log(k)$ SDPs
432 that have to be solved. 433

2) *Numerical Results:* The simulation is set up with 20
434 nodes randomly generated in a square. The results are presented
435 in Fig. 8 with λ_2 as a function of k . The upper bound ob-
436 tained by the relaxation is plotted, as well as all the rounding
437 techniques. 438

It turns out that some techniques may fail to find a solution. In
439 this case, the corresponding values are removed from the figure. 440

It can be seen that the algorithms can achieve the upper
441 bound at the maximum number of edges k_{\lim} . This shows that
442 any algorithm based on edge addition without considering the
443 variable weights is not adapted. 444

Pros and Cons: Each of the methods presented has some
445 advantages and drawbacks. The one that gives the best result is
446 the *step-by-step* method. The fastest is *random fast*. In addition,
447 the method that gives the best tradeoff between speed and value
448 is *log step by step*. 449

450 D. Relaxed SDP With Rounding Algorithm

This algorithm is used to solve relatively small-scale problem
451 when the exhaustive search described in Section III-A fails. 452

- 1) *Golden Section Search:* For a given k , a well-connected
453 network with k edges can now be found. Instead of testing all
454 the possible values of k , the search can be speeded up by con-
455 sidering that algebraic connectivity is a concave function of k . 456

This approximation leads to better results with rounding
457 methods that have good regularity. For large networks, the
458 rounding methods with lower regularity can be used. Instead
459 of computing the value for a given k , a local average value is
460 computed based on three values 461

$$\forall k \in \mathbb{N}, \quad \tilde{f}(k) = \frac{f(k-1) + f(k) + f(k+1)}{3}.$$

As only the value of the connectivity for integer values
462 of k can be computed, it is not possible to use continuous
463 optimization principles. Thus, the golden section search [35] 464

465 is adopted. It consists in creating a decreasing set of intervals
466 containing the optimal value

$$\forall i \in \mathbb{N}, \quad [a_{i+1}, b_{i+1}] \subset [a_i, b_i]$$

467 and $k_{\text{opt}} \in [a_i, b_i]$. Two test values $c_i < d_i$ in $[a_i, b_i]$ facilitate
468 the search. The rules used to update the interval are: 1) $f(c_i) <$
469 $f(d_i) \Rightarrow [a_{i+1}, b_{i+1}] = [c_i, b_i]$ and 2) $f(c_i) > f(d_i) \Rightarrow$
470 $[a_{i+1}, b_{i+1}] = [a_i, d_i]$.

471 At each step, only one new value of f needs to be computed.
472 This new value is usually chosen so that the test values are at
473 the golden ratio $\phi = (1 + \sqrt{5})/2$. Here, the value is rounded
474 to get an integer. This method allows, on average, to divide the
475 length of the interval by ϕ at each step.

476 2) *Relaxed SDP With Rounding Algorithm*: All the steps
477 of the algorithm are summed up. The SDP is solved using
478 the SeDuMi solver [34] and the golden section search. This
479 algorithm that leads to the approximation of the optimum is
480 listed in Algorithm 1.

481 Algorithm 1 Relaxed SDP with step-by-step rounding

```

482 1: Initialize  $a, b$  and  $d$ 
483 2: while  $b - a > 2$  do
484 3:   Choose  $c$  in  $\{(a + d/2), (d + b/2)\}$ 
485 4:   Solve the relaxed SDP with  $k = c$ 
486 5:   for  $p = 1$  to  $k$  do
487 6:      $j \leftarrow \arg \max_i \{x_i | x_i < 1\}$ 
488 7:     Impose  $x_j = 1$ 
489 8:     Solve the SDP
490 9:   end for
491 10:  if  $f(c) < f(d)$  then
492 11:     $a \leftarrow c$ 
493 12:  else
494 13:     $b \leftarrow d, d \leftarrow c$ 
495 14:  end if
496 15: end while
497 16: return  $\lambda_2$ 

```

498 The complexity of this algorithm can be analyzed, which
499 depends on several parameters of the problem. The algorithm
500 uses the step-by-step rounding technique and requires to solve
501 $k + 1$ SDPs for each value of k selected. Each step has a
502 different value for k , and most of them are close to k_{opt} .
503 In addition, there are U such steps. U is defined by
504 $k_{\text{lim}} \phi^{-U} = 1$ since at each step the length of the interval is
505 divided by ϕ . It is obtained that

$$U = \frac{\log(1/k_{\text{lim}})}{\log(1/\phi)}.$$

506 Complexity T also needs to be considered to solve the SDP.
507 T is a polynomial in the size of the entry, which is equivalent to
508 n^2 . Therefore, T is a polynomial function of n .

509 Therefore, the complexity of the whole algorithm can be
510 approximated by $O(k_{\text{opt}} UT)$.

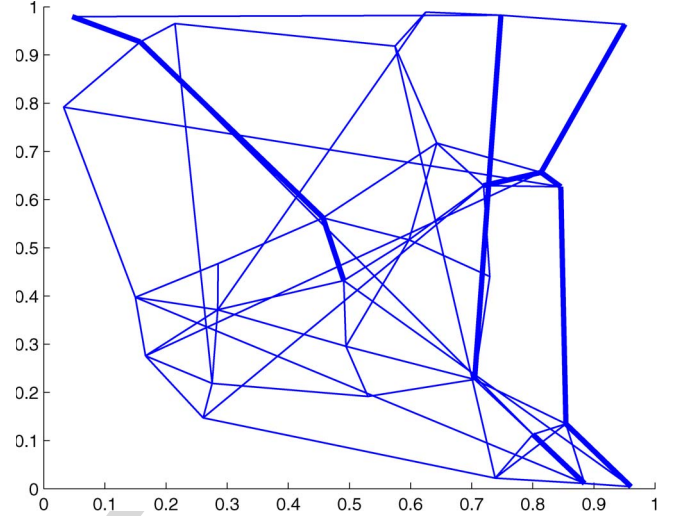


Fig. 9. Optimal result for a 30-node graph.

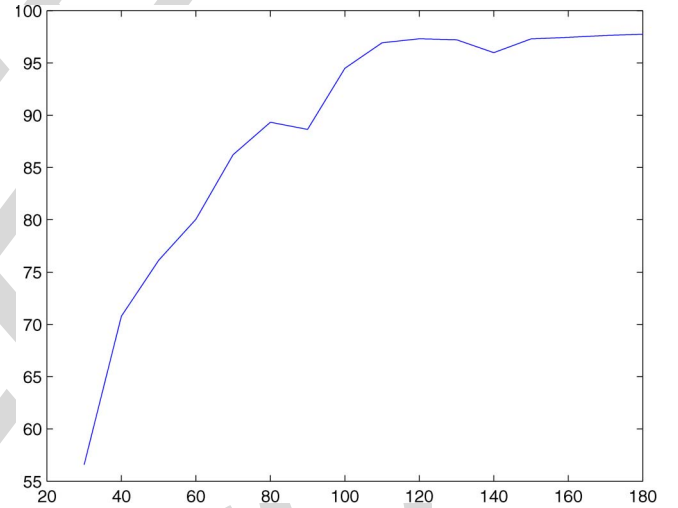


Fig. 10. Values of r for different values of C .

E. Numerical Results

511

512 1) *Optimal Network*: In order to test the full algorithm, a 512
513 set of random nodes is generated in a square. An example of
514 the optimal network for 30 nodes is shown in Fig. 9.

515 The edges that have a weight greater than the lower bound
516 α are represented with a thicker line. In the example in Fig. 9,
517 there are ten edges with a larger weight value than α .

518 2) *Efficiency*: Now, the efficiency of the result is going to
519 be evaluated by comparing the optimal algebraic connectivity
520 to the upper bound. For a given set of nodes, the problem is
521 solved for different values of the total operating cost budget C
522 and the percentage of the solution is computed compared to the
523 bound

$$r = 100 \times \frac{\text{val}(P)}{\text{val}(R)} \%$$

524 The result, as illustrated in Fig. 10, shows that for small
525 values of C , the best result found is very far from the upper

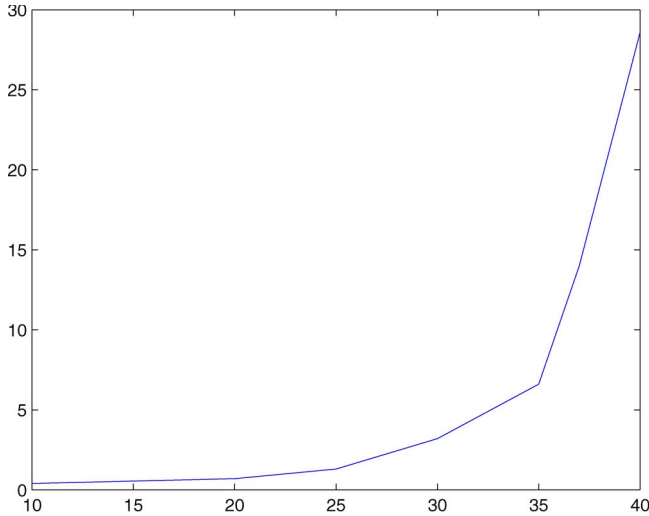


Fig. 11. Time (in seconds) to solve the SDP formulation of the problem for a given number of n nodes.

526 bound. However, when increasing C , the objective value of the
527 problem P quickly increases to reach the value of its relaxed
528 problem R .

529 IV. LARGE-SCALE AIR TRANSPORTATION NETWORKS

530 A. Necessity

531 The method in the previous section is going to be applied to
532 large networks. The most time-consuming computation in the
533 process is solving the SDP. Fig. 11 shows the computational
534 time of solving one SDP for n nodes. It is observed that the
535 running time increases very rapidly. In fact, for n nodes, there
536 are $n(n-1) + 2 \sim n^2$ variables in the SDP. As several SDPs
537 need to be computed in order to solve the problem, it becomes
538 impossible for $n \geq 35$ on the authors' workstation.

539 However, it is necessary to get some results for large values
540 of n because real networks are usually large. For example, the
541 air transportation network contains several hundred nodes when
542 considering the entire USA.

543 B. Cluster Decomposition

544 Since the key factor for operating cost for each link is the
545 route distance (a longer distance route consumes more fuel), the
546 idea in this section is to divide the airports into $g \in \mathbb{N}$ clusters
547 based on the distance between the nodes. These clusters can be
548 solved independently with the relaxed SDP method (Algorithm 1)
549 developed in the previous section and can be connected
550 afterward.

551 To connect the cluster, choose k major nodes in each cluster
552 that will be connected to each other. Then, the problem P has to
553 be solved for these $g \times k$ nodes, except that links between two
554 nodes from the same cluster are not allowed; hence, the graph
555 is not complete.

556 At the end, $g+1$ problems of type (P) need to be solved to
557 get the final result. Fig. 12 shows the idea of the decomposition
558 into several clusters and the selection of major nodes.

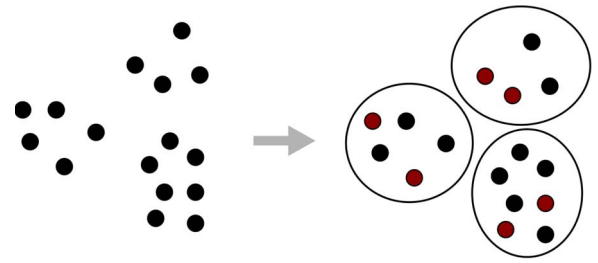


Fig. 12. Set of 16 nodes separated in three clusters with two major nodes in each cluster (in red).

There are several parameters whose values have to be chosen
559 to apply this idea. First, choose the number of clusters and how
560 many major nodes are used in each cluster to connect to other
561 clusters. Second, choose which nodes are kept as major nodes
562 among each cluster. Naturally, it is decided here to take the
563 airports that have the largest traffic demand. 564

In addition, to solve the problem for each small problem $1 \leq$
565 $i \leq g+1$, the value of the maximum operating cost budget C_i
566 in each cluster has to be chosen. A natural option is to choose
567 C_i proportional to the sum s_i of all the costs of the edges in the
568 cluster i and such that $\sum_{i=1}^{g+1} C_i = C$ 569

$$s_i = \sum_{(x,y) \in E} c_{xy},$$

$$C_i = \frac{s_i}{\sum_{j=1}^{g+1} s_j} C.$$

The separation of the nodes into several clusters is made
570 by k -means algorithm [36]. This algorithm has the advantages
571 of being fast, easy to implement, and generally giving good
572 results. 573

To sum up the method described above, the full cluster
574 decomposition algorithm is listed in Algorithm 2. 575

Algorithm 2 Large-scale cluster decomposition

- | | |
|---|-----|
| 1: Initialize g, C_i | 577 |
| 2: k -means algorithm gives g clusters | 578 |
| 3: for $p = 1$ to g do | 579 |
| 4: Solve the cluster problem (with Algorithm 1) | 580 |
| 5: end for | 581 |
| 6: Solve the major node problem (Algorithm 1) | 582 |
| 7: Build the resulting network | 583 |
| 8: return $\lambda_2(L)$ | 584 |
-

C. Evaluation of Efficiency

The goal here is to show that if all $g+1$ clusters are well
586 connected, the resulting graph is well connected too. This
587 depends on the values of some parameters that characterize how
588 each cluster is linked to the others. 589

g clusters are considered. Each cluster has n nodes and k
590 of its nodes are used to connect to other clusters. Let G be
591 the matrix of the graph and F be the vector defined by the
592

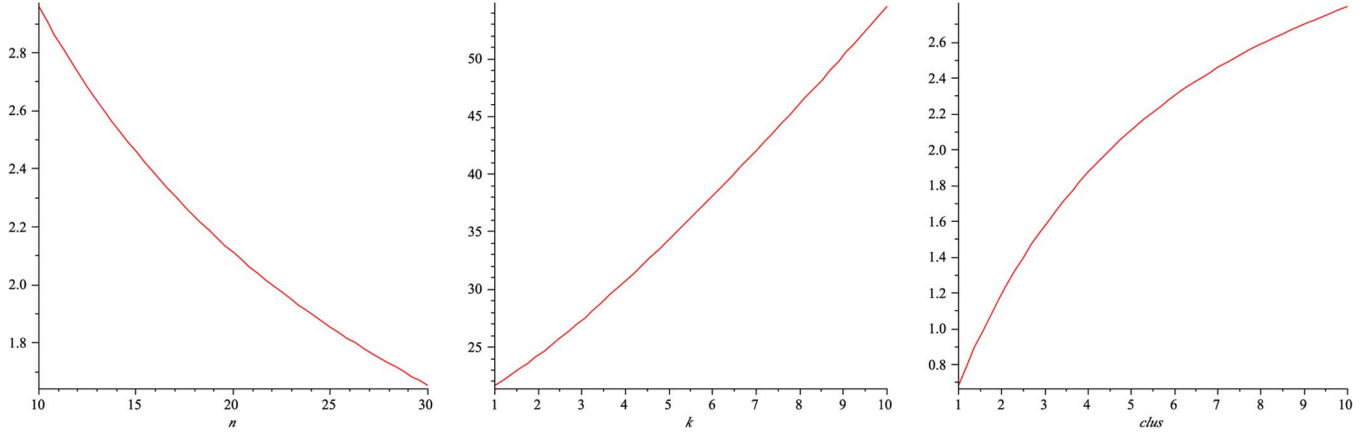


Fig. 13. (a) $\lambda_2 = f(n)$; (b) $\lambda_2 = f(k)$; (c) $\lambda_2 = f(g)$.

593 expression below. If, for instance, $g = 3$, matrix G can be put
594 into the following form:

$$G = \begin{pmatrix} & & & E & 0 & 0 & E & 0 & 0 \\ & A_1 & & 0 & 0 & 0 & 0 & 0 & 0 \\ & & & 0 & 0 & 0 & 0 & 0 & 0 \\ E & 0 & 0 & & & & E & 0 & 0 \\ 0 & 0 & 0 & & A_2 & & 0 & 0 & 0 \\ 0 & 0 & 0 & & & & 0 & 0 & 0 \\ E & 0 & 0 & E & 0 & 0 & & & \\ 0 & 0 & 0 & 0 & 0 & 0 & & A_3 & \\ 0 & 0 & 0 & 0 & 0 & 0 & & & \end{pmatrix}$$

$$F = \begin{pmatrix} \alpha e \\ \beta e \\ \frac{\beta e}{0} \\ 0 \\ 0 \\ -\alpha e \\ -\beta e \\ -\beta e \end{pmatrix}$$

595 with the following notation. e is the all-one vector. α and β are
596 constants that will be computed in the next paragraph. A_1 , A_2 ,
597 and A_3 represent the adjacency matrices of the three clusters.
598 E is a $k \times k$ matrix with all elements equal to 1.

599 1) *Fiedler Vector*: The Fiedler vector is the vector solution
600 of the minimization problem

$$\min_{x \in \mathbb{R}^n} \{x^T Lx \mid \|x\| = 1, \quad xe = 0\}.$$

601 It is known to be an indicator on how to split a graph into two
602 smaller graphs. In fact, the nodes that have the same sign in this
603 vector form a cut of the graph (see [37]).

604 Here, the optimal cut will naturally be found between two
605 clusters. Since some of the nodes play the same role, the Fiedler
606 vector has a shape close to F where α and β are constants that
607 need to be determined.

608 This assumption has been verified by numerical experiments
609 and it seems to be a very good approximation of the real Fiedler
610 vector.

611 2) *Computing the Connectivity*: Consider that the Fiedler
612 vector has the form of F and matrices are full, which means

all nondiagonal elements are equal to 1. The matrix products
613 give
614

$$\lambda_2 = F^T L F,$$

$$\lambda_2 = 2k\alpha X + 2(n-k)\beta Y$$

with

$$X = \alpha(n-1+k(g-1)) - (k-1)\alpha - (n-k)\beta + k\alpha,$$

$$Y = \beta(n-1) - k\alpha - (n-k-1)\beta.$$

It is also known that $\|F\| = 1$; thus

$$2k\alpha^2 + (2n-2k)\beta^2 = 1,$$

$$\alpha = \sqrt{\frac{1 - (2n-2k)\beta^2}{2k}}.$$

Substitute α with this expression and β is given by the

$$\frac{d\lambda_2}{d\beta} = 0. \tag{7}$$

615 With a computation software package like Maple, this gives
616
617
618
619

$$\lambda_2 = f(n, k, g).$$

3) *Resulted Curves*: By solving (7), the values of α , β , and
620 λ_2 are obtained. The following figures have been obtained with
621 Maple. Among the three parameters k , g , and n , fix two of them
622 and let the third one vary to see its influence on connectivity.
623

Fig. 13 provides a clearer idea on how to choose the value
624 of each parameter. For example, connectivity is almost linear
625 regarding k but has a concave shape when represented as a
626 function of the number of clusters g .
627

There exists a tradeoff: If g is too large, kg will be too large to
628 be solved. On the contrary, if g is too small, each of the cluster
629 will have too many nodes to be solved.
630

4) *Numerical Results*: The data used are the 100 largest
631 cities in the United States. Fig. 14 shows the 100 biggest
632 cities without any link. The cluster decomposition is used to
633 divide these 100 cities into $g = 5$ groups. In each group, we
634 selected $k = 5$. The lower bound $\alpha = 2$ and the upper bound
635

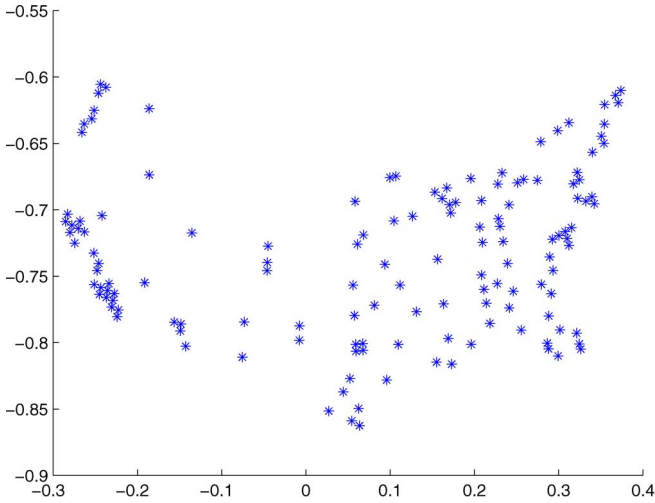


Fig. 14. Shown are the 100 largest cities in the USA.

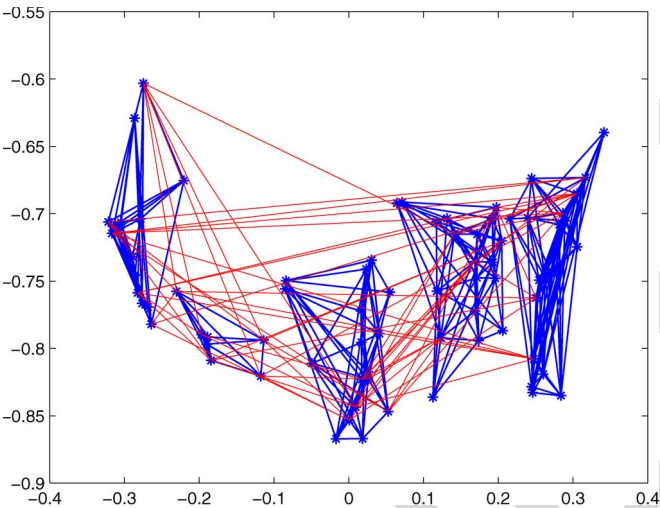


Fig. 15. Result for the 100 largest cities in the USA.

636 $\beta = 10$. The total running time is 317 s with MATLAB on our
637 workstation. The algebraic connectivity that we have achieved
638 is $\lambda_2 = 2.6$.

639 The optimal network found is illustrated in Fig. 15. The blue
640 lines represent the edges inside each cluster and the red lines
641 represent the edges that connect nodes from different clusters.

642 In a real network, most airlines use spoke-hub planning, in
643 which the regional airports are clustered and connected to their
644 regional hub airport. Fig. 15 shows the same behavior that
645 regional airports are clustered together. In a real network in the
646 United States, the number of the major nodes k for each cluster
647 is usually 1, which means that the hub airport is the only major
648 node for its cluster. In a real network in Europe, the number of
649 the major nodes k is usually bigger than 1. In fact, the number
650 k in a European network is those hub airports in each country.
651 For example, Air France has hubs at Paris and Lyon ($k = 2$)
652 and Air Berlin has its hubs at Berlin, Düsseldorf, Hamburg, and
653 Munich ($k = 4$). In summary, the result in Fig. 15 is a practical
654 design, and more importantly, the computation is very efficient
655 for large-scale network planning.

V. DIRECTED AIR TRANSPORTATION NETWORK 656

A. From Undirected Graph to Directed Graph 657

In this section, the methods are extended in directed graphs. 658
In order to be consistent with the undirected case, the graphs 659
need to be balanced, which means that the number of aircraft 660
that comes in is the same as the number of aircraft that leaves 661
the airport 662

$$\forall i \in \{1, \dots, n\}, \quad \sum_{j=1}^n w_{ij} = \sum_{k=1}^n w_{ki}.$$

It is clear that the set of undirected graphs is included in the set 663
of directed balanced graphs. Therefore, the results should be at 664
least as good as in the previous section. 665

Definition: According to [38], if $\Omega = \{x \in \mathbb{R}^n, xe = 666$
 $0, \|x\| = 1\}$, the definition of the algebraic connectivity can be 667
extended for directed balanced graphs with 668

$$\min_{x \in \Omega} x^T L x = \lambda_2 \left(\frac{1}{2} (L + L^T) \right).$$

Property 4: In the directed case and with this definition 669
of the algebraic connectivity, the upper bound given by the 670
continuous relaxation is the same as in the undirected case. 671

Proof: Given the optimum directed balanced graph in the 672
relaxed problem and its incidence matrix G , H can be created 673

$$H = \frac{G + G^T}{2}$$

where H is symmetric and satisfies all the constraints of the 674
problem since they are linear. In addition with the definition of 675
the connectivity for directed graphs, the connectivity of H is 676
clearly the same as the connectivity of G . 677

Since it is also known that undirected graphs are a subset of 678
directed balanced graphs, the bounds are equal in both cases. 679
This will allow us to easily evaluate the improvement brought 680
by directed graphs. ■ 681

B. Results 682

The same method is used as in Section III. The results are 683
impressively better with directed graphs, as shown in Fig. 16. 684
The best value for the directed balanced case almost reached 685
the upper bound. It is also noticed that the optimal result has 686
less edges than the optimal network in the undirected case (an 687
edge in the undirected case is counted in both ways). 688

It is shown in Fig. 17 that most of the edges in the optimal 689
solution are oriented in only one way, which shows that the 690
solution is very different from the undirected case. 691

However, there is an important drawback. Indeed, two times 692
as many variables are needed for directed networks. Thus, the 693
problem takes a much longer time to be solved and is only 694
applicable on smaller networks. 695

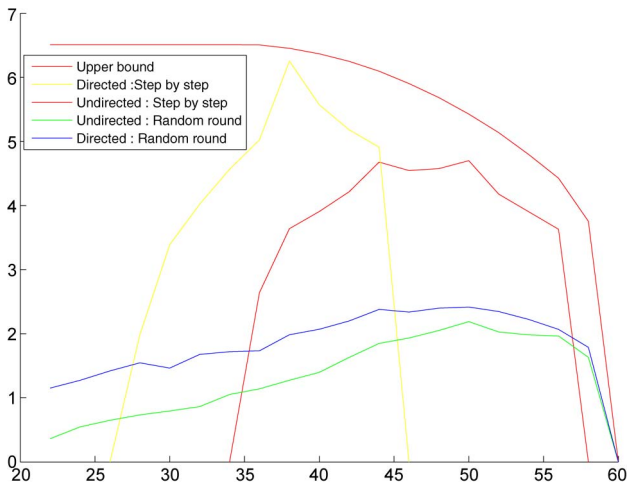


Fig. 16. $\lambda = f(k)$ for the same graph with different approaches.

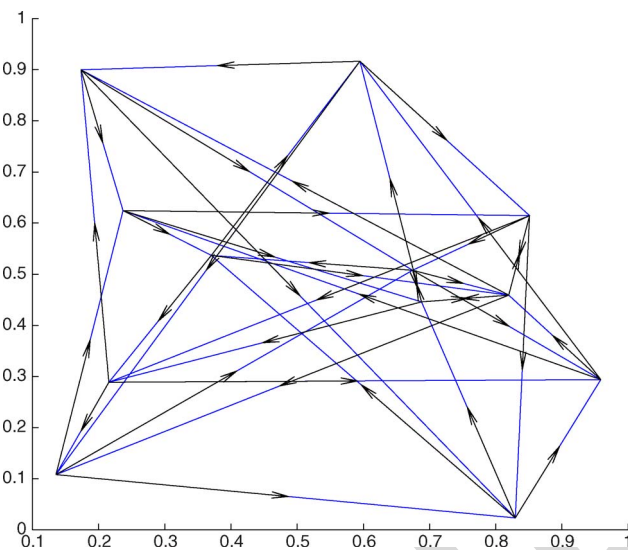


Fig. 17. Optimal directed graph.

696 C. Failure Case

697 If an edge or a node is removed, the graph is not balanced
698 anymore. This can cause important problems in practice; hence,
699 the remaining weights in the graph need to be changed to handle
700 this problem.

701 This operation can be done by using a flow algorithm. The
702 first step is to link the nodes with positive aircraft balance to a
703 virtual source and those with negative balance to a sink. The ca-
704 pacities of these links are equal to the absolute value of the
705 difference in the balance flow for the node. The capacity of the
706 other links of the graph is β .

707 Then, consider the problem of the maximization of the flow
708 from the source to the sink. This problem can be solved by using
709 Edmonds–Karp algorithm [39], which has efficient complexity,
710 i.e., $O(nm^2)$. This algorithm maintains the balance of the flow
711 at each node.

712 At the end, the graph is the graph solution of the flow
713 problem when the source and the sink are removed. Figs. 18
714 and 19 show an example of a graph in which a node is removed,

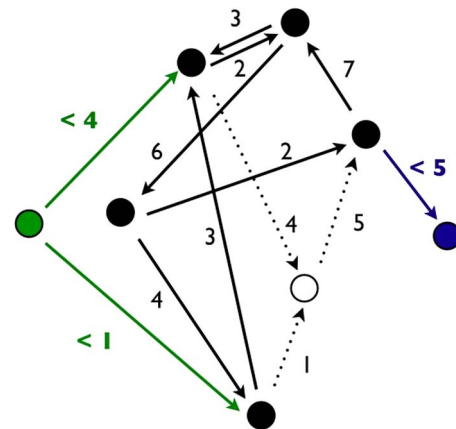


Fig. 18. Example of a graph with a node failure.

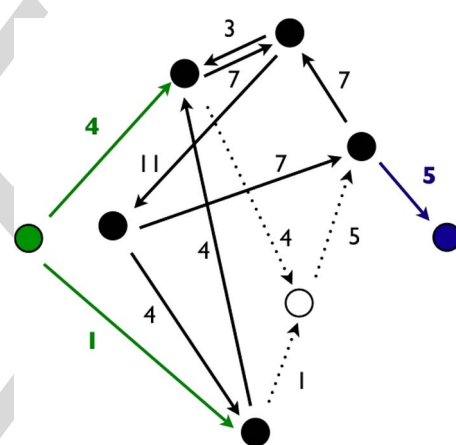


Fig. 19. Example of a graph after maximization of the flow.

before and after maximization of the flow. The graph in Fig. 19
715 is now balanced by Edmonds–Karp algorithm after removing 716
the source (green node) and the sink (blue node). 717

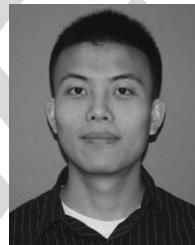
VI. CONCLUSION

In this paper, a new problem concerning the maximization of
719 the algebraic connectivity of a network has been presented and
720 studied. This problem consists of finding both the edges of the
721 graph and their weight assignment under several constraints. 722
First, the problem in small networks is exactly solved, and it is
723 shown that the problem cannot be separated into two already
724 studied independent problems. Then, a relaxed SDP method
725 with step-by-step rounding is presented to solve the problem
726 approximately for better computational efficiency. With the
727 method developed for small-scale network, the cluster decom-
728 position method is proposed to solve the large-scale network
729 problem and successfully find the near-optimal solution for a
730 network of the 100 largest cities in the United States. Finally,
731 the study is extended to directed graphs. Numerical experiments
732 and analysis are performed for all the proposed algorithms. The
733 developed methods are able to model and maximize robustness
734 in air transportation networks for airlines and for the NAS. They
735 also provide an option to improve current ways of the generic
736 network design. 737

738

REFERENCES

- [1] R. Guimera and L. Amaral, "Modeling the world-wide airport network," *Eur. Phys. J. B, Condens. Matter Complex Syst.*, vol. 38, no. 2, pp. 381–385, Mar. 2004.
- [2] R. Kincaid, N. Alexandrov, and M. Holroyd, "An investigation of synchrony in transport networks," *Complexity*, vol. 14, no. 4, pp. 34–43, Mar./Apr. 2008.
- [3] E. Vargo, R. Kincaid, and N. Alexandrov, "Towards optimal transport networks," *J. Syst., Cybern. Inf.*, vol. 8, no. 4, pp. 59–64, Jul. 2010.
- [4] International Civil Aviation Organization (ICAO), "Procedures for air navigation services—Rules of the air and air traffic services," Montréal, QC, Canada, doc 4444-RAC/501, 2010.
- [5] P. Kostiuk, D. Lee, and D. Long, "Closed loop forecasting of air traffic demand and delay," presented at the 3rd USA/Europe Air Traffic Management R&D Seminar, Napoli, Italy, Jun. 2010, Paper 80.
- [6] K. Nam and T. Schaefer, "Forecasting international airline passenger traffic using neural networks," *Logist. Transp. Rev.*, vol. 31, no. 3, pp. 239–251, Sep. 1995.
- [7] F. Alamdari and S. Fagan, "Impact of the adherence to the original low cost model on the profitability of low cost airlines," *Transp. Rev.*, vol. 25, no. 3, pp. 377–392, May 2005.
- [8] M. Dresner, J.-S. C. Lin, and R. Windle, "The impact of low-cost carriers on airport and route competition," *J. Transp. Econ. Policy*, vol. 30, no. 3, pp. 309–328, Sep. 1996.
- [9] K. Button and S. Lall, "The economics of being an airport hub city," *Res. Transp. Econ.*, vol. 5, pp. 75–105, 1999.
- [10] T. Oum, A. Zhang, and Y. Zhang, "A note on optimal airport pricing in a hub-and-spoke system," *Transp. Res. B, Methodol.*, vol. 30, no. 1, pp. 11–18, Feb. 1996.
- [11] X.-B. Hu, W.-H. Chen, and E. Di Paolo, "Multi-airport capacity management: Genetic algorithm with receding horizon," *IEEE Trans. Intell. Transp. Syst.*, vol. 8, no. 2, pp. 254–263, Jun. 2007.
- [12] X.-B. Hu and E. Di Paolo, "Binary-representation-based genetic algorithm for aircraft arrival sequencing and scheduling," *IEEE Trans. Intell. Transp. Syst.*, vol. 9, no. 2, pp. 301–310, Jun. 2008.
- [13] Y. Eun, I. Hwang, and H. Bang, "Optimal arrival flight sequencing and scheduling using discrete airborne delays," *IEEE Trans. Intell. Transp. Syst.*, vol. 11, no. 2, pp. 359–373, Jun. 2010.
- [14] Z.-H. Zhan, J. Zhang, Y. Li, O. Liu, S. Kwok, W. Ip, and O. Kaynak, "An efficient ant colony system based on receding horizon control for the aircraft arrival sequencing and scheduling problem," *IEEE Trans. Intell. Transp. Syst.*, vol. 11, no. 2, pp. 399–412, Jun. 2010.
- [15] *FlightStats-Global Flight Tracker, Status Tracking and Airport Information*, FlightStats, Inc., Portland, OR, USA, 2013, retrieved on March 16, 2013. [Online]. Available: <http://www.flightstats.com>
- [16] Federal Aviation Administration (FAA), "FAA Aerospace Forecasts FY 2008–2025," Washington, DC, USA, Dec. 2010.
- [17] S. Conway, "Scale-free networks and commercial air carrier transportation in the United States," in *Proc. 24th Int. Congr. Aeron. Sci.*, Yokohama, Japan, 2004, pp. 1–12.
- [18] P. A. Bonnefoy, "Scalability of the air transportation system and development of multi-airport systems: A worldwide perspective," Ph.D. dissertation, MIT, Cambridge, MA, USA, Jun. 2008.
- [19] N. Alexandrov, "Transportation network topologies," NASA Langley Res. Center, Hampton, VA, USA, Tech. Rep., 2004.
- [20] T. Kotegawa, D. DeLaurentis, K. Noonan, and J. Post, "Impact of commercial airline network evolution on the US air transportation system," in *Proc. 9th USA/Europe ATM Res. Develop. Semin.*, Berlin, Germany, 2011.
- [21] A. Bigdeli, A. Tizghadam, and A. Leon-Garcia, "Comparison of network criticality, algebraic connectivity, and other graph metrics," presented at the 1st Annu. Workshop Simplifying Complex Network Practitioners, Venice, Italy, 2009, Paper 4.
- [22] A. Jamakovic and S. Uhlig, "On the relationship between the algebraic connectivity and graph's robustness to node and link failures," in *Proc. 3rd EuroNGI Netw. Conf.*, May 2007, pp. 96–102.
- [23] A. Jamakovic and P. V. Mieghem, "On the robustness of complex networks by using the algebraic connectivity," in *Proc. Netw. Ad Hoc Sensor Netw., Wireless Netw., Next Gen. Internet*, A. Das, H. K. Pung, F. Bu Sung Lee, and L. Wong Wai Choong, Eds., 2008, pp. 183–194.
- [24] R. H. Byrne, J. T. Feddema, and C. T. Abdallah, "Algebraic connectivity and graph robustness," Sandia Nat. Lab., Albuquerque, NM, USA, Tech. Rep., Jul. 2009.
- [25] P. Wei and D. Sun, "Weighted algebraic connectivity: An application to airport transportation network," in *Proc. 18th IFAC World Congress*, Milan, Italy, Aug. 2011, pp. 13 864–13 869.
- [26] A. Ghosh and S. Boyd, "Growing well-connected graphs," in *Proc. 45th IEEE Conf. Decis. Control*, Dec. 2006, pp. 6605–6611.
- [27] J. Sun, S. Boyd, L. Xiao, and P. Diaconis, "The fastest mixing Markov process on a graph and a connection to a maximum variance unfolding problem," *SIAM Rev.*, vol. 48, no. 4, pp. 681–699, Nov. 2006.
- [28] F. Goring, C. Helmsberg, and M. Wappler, "Embedded in the shadow of the separator," *SIAM J. Optim.*, vol. 19, no. 1, pp. 472–501, Feb. 2008.
- [29] S. Boyd, "Convex optimization of graph Laplacian eigenvalues," in *Proc. Int. Congr. Math.*, 2006, vol. 3, pp. 1311–1319.
- [30] S. Boyd, P. Diaconis, and L. Xiao, "Fastest mixing Markov chain on a graph," *SIAM Rev.*, vol. 46, no. 4, pp. 667–689, Dec. 2004.
- [31] M. Fiedler, "Algebraic connectivity of graphs," *Czechoslovak Math. J.*, vol. 23, no. 98, pp. 298–305, 1973.
- [32] B. Mohar, "The Laplacian spectrum of graphs," in *Graph Theory, Combinatorics, and Applications*. New York, NY, USA: Wiley, 1991, pp. 871–898.
- [33] M. Siotani, "Some applications of Loewner's ordering on symmetric matrices," *Ann. Inst. Stat. Math.*, vol. 19, no. 1, pp. 245–259, Dec. 1967.
- [34] J. F. Sturm, "Using SeDuMi 1.02, A Matlab toolbox for optimization over symmetric cones," *Optim. Methods Softw.*, vol. 11, no. 1–4, pp. 625–653, Jan. 1999.
- [35] W. Press, S. Teukolsky, W. Vetterling, and B. Flannery, *The Art of Scientific Computing*, 3rd ed. Cambridge, U.K.: Cambridge Univ. Press, 2007, ch. Section 10.2. Golden Section Search in One Dimension, pp. 492–496.
- [36] J. Kleinberg and E. Tardos, *Algorithm Design*. Reading, MA, USA: Addison-Wesley, 2005, ch. 4.7 Clustering, pp. 157–161.
- [37] S. Martinez, G. Chatterji, D. Sun, and A. Bayen, "A weighted graph approach for dynamic airspace configuration," presented at the AIAA Conf. Guidance, Control Dynamics, Hilton Head, SC, USA, Aug. 2007, Paper AIAA 2007-6448.
- [38] C. Wu, "Algebraic connectivity of directed graphs," *Linear Multilinear Algebra*, vol. 53, no. 3, pp. 203–223, Jun. 2005.
- [39] T. H. Cormen, C. E. Leiserson, R. L. Rivest, and C. Stein, *Introduction to Algorithms*. Cambridge, MA, USA: MIT Press, 2009, ch. 26.2 The Ford-Fulkerson method, pp. 727–730.



Peng Wei (M'12) received the Bachelor's degree in automation from Tsinghua University, Beijing, China; the Master's degree in electrical engineering from Stony Brook University, Stony Brook, NY, USA; and the Ph.D. degree in aerospace engineering from Purdue University, West Lafayette, IN, USA.

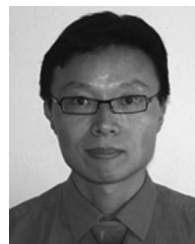
He is an Operations Research Consultant with American Airlines, Fort Worth, TX, USA. His research interests include next-generation air transportation system, environmental impact of aviation and unmanned aerial vehicle integration in the National Airspace System.

Dr. Wei received the Purdue College of Engineering Outstanding Research Award in 2013.



Gregoire Spiers received the Bachelor's degree in applied mathematics from École Polytechnique, Palaiseau, France, in 2012.

He was a Visiting Student with Purdue University, West Lafayette, IN, USA, in 2011. He is currently a Research Engineer with Amadeus S.A.S., Sophia Antipolis, France.



Dengfeng Sun (M'08) received the Bachelor's degree in precision instruments and mechatronics from Tsinghua University, Beijing, China; the Master's degree in industrial and systems engineering from The Ohio State University, Columbus, OH, USA; and the Ph.D. degree in civil engineering from University of California, Berkeley, CA, USA.

He is an Assistant Professor with the School of Aeronautics and Astronautics, Purdue University, West Lafayette, IN, USA. His research interests include control and optimization, with an emphasis on applications in air traffic flow management, dynamic airspace configuration and studies for the next-generation air transportation system.

AQ4

AUTHOR QUERIES

AUTHOR PLEASE ANSWER ALL QUERIES

AQ1 = Please provide keywords.

AQ2 = Please check if changes made in the affiliation note of author Gregoire Spiers are appropriate, with reference to the given biography. Please also check accuracy of postal code and location.

AQ3 = Please provide page range in Ref. [20].

AQ4 = Please check accuracy of provided location.

END OF ALL QUERIES

IEEE
Proof

Algebraic Connectivity Maximization for Air Transportation Networks

Peng Wei, *Member, IEEE*, Gregoire Spiers, and Dengfeng Sun, *Member, IEEE*

Abstract—It is necessary to design a robust air transportation network. An experiment based on the real air transportation network is performed to show that algebraic connectivity is a fair measure for network robustness under random failures. Therefore, the goal of this paper is to maximize algebraic connectivity. Some researchers solve the maximization of the algebraic connectivity by choosing the weights for the edges in the graph. Others focus on the best way to add edges in a network in order to optimize the connectivity. In this paper, the authors formulate a new air transportation network model and show that the corresponding algebraic connectivity optimization problem is interesting because the two subproblems of adding edges and choosing edge weights cannot be treated separately. The new problem is formulated and exactly solved in a small air transportation network case. The authors also propose the approximation algorithm in order to achieve better efficiency. For large networks, the semidefinite programming with cluster decomposition is first presented. Moreover, the algebraic connectivity maximization for directed networks is discussed. Simulations are performed for a small-scale case, large-scale problem, and directed network problem.

Index Terms—Author, please supply index terms/keywords for your paper. To download the IEEE Taxonomy go to http://www.ieee.org/documents/Taxonomy_v101.pdf.

I. INTRODUCTION

AN AIR transportation network consists of distinct airports (cities) and direct flight routes between airport pairs [1]. Usually, a graph $G(V, E)$ is used to describe an air transportation network [2], [3], where the node set V represents all the n airports and the edge (link) set E represents all the m direct flight routes between airports. If a direct flight route from airport a to airport b exists, normally, the direct return route from airport b to airport a also exists [4]; $G(V, E)$ is constructed as an undirected simple graph, where the airports are indexed as $\{v_i | i = 1, 2, \dots, n\}$ and the direct flight routes are named as e_{ij} if there is a direct route between airports v_i and v_j . There are many factors to be considered when designing an air transportation network, such as traffic demand, operating cost, airport hubs, market competition, multiairport systems, and

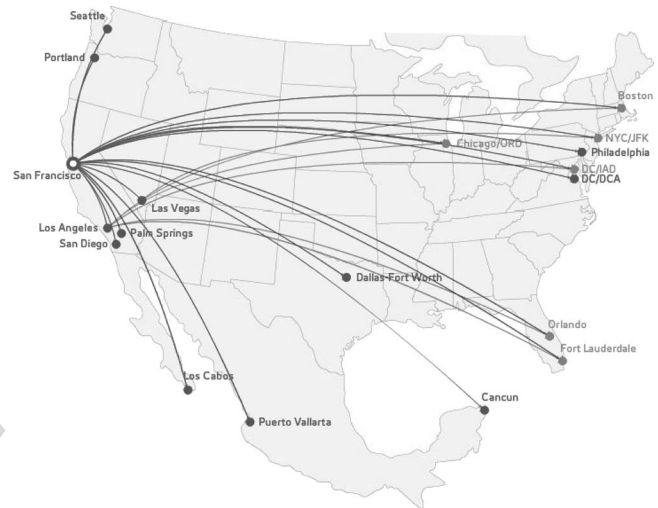


Fig. 1. Air transportation network route map for Virgin America Airlines.

scheduling [5]–[14]. In this paper, we focus on investigating the network robustness maximization, particularly the algebraic connectivity maximization.

A. Algebraic Connectivity and Air Transportation Network Robustness

In order to illustrate the relationship between the algebraic connectivity and air transportation network robustness, a real air transportation network of Virgin America is studied. The following experiment shows that algebraic connectivity is a fair measurement for the network robustness with regard to random link failures under the current Virgin America network topology.

According to the current route map of Virgin America in Fig. 1, we consider the 16 airports in the United States and obtain the adjacency matrix as Table I. The 16 United States airports include Boston (BOS), New York City/John F. Kennedy (JFK), Philadelphia, Washington Dulles International Airport (DC/IAD), Ronald Reagan Washington National Airport (DC/DCA), Chicago O’Hare International Airport (ORD), Orlando, Fort Lauderdale, Dallas/Fort Worth, Seattle, Portland, San Francisco, Los Angeles, Las Vegas, San Diego, and Palm Springs and are indexed as numbers 1–16. San Francisco International Airport (SFO) and Los Angeles International Airport (LAX) are two major hubs of the entire network. Both have at least one direct flight to almost all the other airports.

In order to show how well the algebraic connectivity can measure the robustness of an air transportation network, we

Manuscript received November 6, 2012; revised April 5, 2013 and August 20, 2013; accepted October 1, 2013. The Associate Editor for this paper was J.-P. B. Clarke.

P. Wei is with the Operations Research and Advanced Analytics, American Airlines, Fort Worth, TX 76155 USA (e-mail: peng.wei@aa.com).

G. Spiers was with the Department of Applied Mathematics, École Polytechnique, 91120 Palaiseau, France. He is now with Amadeus S.A.S., 06902 Sophia Antipolis, France (e-mail: gregoire.spiers@polytechnique.org).

D. Sun is with the School of Aeronautics and Astronautics, Purdue University, West Lafayette, IN 47907 USA (e-mail: dsun@purdue.edu).

Color versions of one or more of the figures in this paper are available online at <http://ieeexplore.ieee.org>.

Digital Object Identifier 10.1109/TITS.2013.2284913

TABLE I
ADJACENCY MATRIX CONSISTS OF 16 VIRGIN AMERICA AIRLINES AIRPORTS IN THE USA

	1	2	3	4	5	6	7	8	9	10	11	12	13	14	15	16
1	0	0	0	0	0	0	0	0	0	0	0	1	1	0	0	0
2	0	0	0	0	0	0	0	0	0	0	0	1	1	1	0	0
3	0	0	0	0	0	0	0	0	0	0	0	1	1	0	0	0
4	0	0	0	0	0	0	0	0	0	0	0	1	1	0	0	0
5	0	0	0	0	0	0	0	0	0	0	0	1	0	0	0	0
6	0	0	0	0	0	0	0	0	0	0	0	1	1	0	0	0
7	0	0	0	0	0	0	0	0	0	0	0	1	1	0	0	0
8	0	0	0	0	0	0	0	0	0	0	0	1	1	0	0	0
9	0	0	0	0	0	0	0	0	0	0	0	1	1	0	0	0
10	0	0	0	0	0	0	0	0	0	0	0	1	1	0	0	0
11	0	0	0	0	0	0	0	0	0	0	0	1	1	0	0	0
12	1	1	1	1	1	1	1	1	1	1	1	0	1	1	1	1
13	1	1	1	1	0	1	1	1	1	1	1	1	0	0	0	0
14	0	1	0	0	0	0	0	0	0	0	0	1	0	0	0	0
15	0	0	0	0	0	0	0	0	0	0	0	1	0	0	0	0
16	0	0	0	0	0	0	0	0	0	0	0	1	0	0	0	0

69 created six different *weighted air transportation networks* with
70 the same topology in Table I by randomly assigning one of
71 the three types of *link weights* to each route. Each link weight
72 is an indication of link strength. A larger weight represents a
73 stronger link and a smaller weight shows that the corresponding
74 link is easier to fail. There are many reasons for route failure,
75 such as weather disturbance, long ground delay program, long
76 airspace flow program (AFP), aircraft mechanical problem, and
77 upline flight delay/cancellation. The route failure rate statis-
78 tics are published by each origin–destination pair (route) and
79 different routes have different features [15]. For example, the
80 route failure rate between JFK and BOS during summer is
81 higher than that between SFO and LAX because of the crowded
82 northeastern airspace (AFP is more frequent) and more summer
83 thunderstorms. Another example is that a shorter route is easier
84 to fail than a longer transcontinental route because: 1) airlines
85 usually put larger aircraft on transcontinental route, and these
86 aircraft are more robust to weather disturbance and 2) airlines
87 are more likely to cancel shorter route flights because the flight
88 frequency on a shorter route is higher; therefor, the passengers
89 on the canceled flight are easier to protect (be reaccommodated
90 to later flights). In summary, each route has its own features
91 and thus in our model we consider that they have different
92 possibilities for failure.

93 The three types of link weights are mapped to different link
94 failure probabilities (see Table II). The link failure probability
95 range [%0, %5] is obtained from the historical flight cancellation
96 rate between September 15, 2012, and November 15, 2012 [15].
97 A network failure is defined as the existence of at least one
98 pair of nodes that cannot access each other through any one or
99 multiple links. For each one of the six weighted networks, 1000
100 trials are performed. In each trial, every link fails randomly

TABLE II
MAPPING BETWEEN LINK WEIGHTS AND LINK FAILURE PROBABILITIES

link weight w_{ij}	1	2	3
link failure probability	5%	3%	1%

TABLE III
NETWORK FAILURE NUMBERS WITH DIFFERENT ALGEBRAIC
CONNECTIVITY VALUES

algebraic connectivity	total failures in 10000 trials
1.0306	1113
1.7586	991
1.8661	763
1.9711	571
2.3128	423
2.7393	355

according to the failure probabilities listed in Table II. The total
101 number of network failures is counted in 1000 random trials.
102 The results are shown in Table III with algebraic connectivity
103 sorted in ascending order.
104

We can see that with higher algebraic connectivity, the
105 network is more robust and has fewer network failures. With
106 lower weighted algebraic connectivity, the network is easier to
107 break down. Therefor, algebraic connectivity is a fair robustness
108 measure for the air transportation network, and we need to find
109 the maximized algebraic connectivity.
110

The air traffic demand is expected to continue its rapid
111 growth in the future. The Federal Aviation Administration
112 estimated that the number of passengers is projected to increase
113 by an average of 3% every year until 2025 [16]. The expanding
114 traffic demand on the current air transportation networks of
115 different airlines will cause more and more flight cancellations
116 with the limited airport and airspace capacities. As a result,
117 more robust air transportation networks are desired to sustain
118

119 the increasing traffic demand for each airline and for the entire
120 National Airspace System (NAS). This is the major motivation
121 of this paper.

122 B. Related Work

123 An air transportation network and its robustness have been
124 studied over the last several years. Guimera and Amaral first
125 studied the scale-free graphical model of the air transportation
126 network [1]. Conway showed that it was better to describe
127 the national air transportation system or the commercial air
128 carrier transportation network as a system of systems [17].
129 Bonnefoy showed that the air transportation network was scale
130 free with aggregating multiple airport nodes into meganodes
131 [18]. Alexandrov defined that on-demand transportation net-
132 works would require robustness in system performance [19].
133 The robustness of an on-demand network would depend on the
134 tolerance of the network to variability in temporal and spatial
135 dynamics of weather, equipment, facility, crew positioning, etc.
136 Kotegawa *et al.* surveyed different metrics for air transportation
137 network robustness, including betweenness, degree, centrality,
138 connectivity, etc. [20]. They selected clustering coefficient and
139 eigenvector centrality as the network robustness metrics in
140 their machine learning approach. Bigdeli *et al.* compared alge-
141 braic connectivity, network criticality, average degree, average
142 node betweenness, and other metrics [21]. Jamakovic *et al.*
143 found that algebraic connectivity was an important metric in
144 the analysis of various robustness problems in several typical
145 network models [22], [23]. Byrne *et al.* showed that algebraic
146 connectivity was the efficient measure for the robustness of
147 both small and large networks [24]. Vargo *et al.* in [3] chose
148 algebraic connectivity as the robustness metric and built the
149 optimization problem solved by the edge swapping-based tabu
150 search algorithm.

151 In this paper, we measure the robustness of air transportation
152 network by computing the algebraic connectivity, which is
153 usually considered as one of the most reasonable and efficient
154 evaluation methods [24], [25]. Although the maximized value
155 of algebraic connectivity is abstract, the optimized air trans-
156 portation network structure and weighting assignment provide
157 us the applicable design.

158 There are some literature on algebraic connectivity maxi-
159 mization. The problems studied can be divided into two cat-
160 egories, namely, the edge addition problem and the variable
161 weights problem.

- 162 1) **Edge addition problem:** The goal is to add or remove a
163 given number of k edges on a graph in order to get the best
164 algebraic connectivity. The edges to be added or removed
165 are selected from a candidate set. The algorithms that
166 have been developed to solve the problem include tabu
167 search [25], greedy algorithms [25], [26], and rounded
168 semidefinite programming (SDP) [26].
- 169 2) **Variable weights problem:** The edges of the graph are
170 fixed and the goal is to determine the edge weights in
171 order to maximize the algebraic connectivity. This is
172 a convex optimization problem that is often solved by
173 using an SDP formulation [27]–[29] or a subgradient
174 algorithm [30].

C. Contribution

175

The major contribution of this paper compared with what
176 has been studied is that we find that, in order to maximize
177 the algebraic connectivity, the edge addition problem and the
178 variable weights problem cannot be studied separately. Solving
179 one of them independently will only result in a suboptimal
180 solution. Therefore, we propose a new algorithm to solve both
181 problems at the same time. How to choose the edges of the
182 graph is demonstrated, as well as how to assign their weights.
183 In addition, we are the first to present the cluster decomposition
184 method to achieve better computation efficiency for large-scale
185 networks. We are also the first to discuss the algebraic connec-
186 tivity maximization for directed air transportation networks. 187

The rest of this paper is structured as follows. Section II
188 shows why this problem naturally arises in air transportation
189 networks and how it can be formulated. In Section III, the
190 problem is exactly solved for small networks, and the fact that
191 the two problems are not independent is highlighted. Then, the
192 authors present the SDP formulation and the more efficient full
193 algorithm, which includes relaxed SDP, and solution rounding
194 is proposed. In Section IV, the problem for large networks
195 is solved, the computational efficiency is analyzed, and the
196 numerical results are provided. The algebraic connectivity op-
197 timization for directed air transportation networks is presented
198 in Section V. Section VI concludes this paper. 199

II. PROBLEM FORMULATION

200

A graph G with n nodes and m edges is used to define an air
201 transportation network. Let $A = (a_{ij})$ be the adjacency matrix
202 of G . The Laplacian matrix $L = (l_{ij})$ of G is defined by 203

$$\begin{cases} l_{ij} = -a_{ij}, & \text{if } i \neq j \\ l_{ii} = \sum_{j=1}^n a_{ij}. \end{cases}$$

The eigenvalues of L are sorted $\lambda_1 \leq \lambda_2 \leq \dots \leq \lambda_n$. L is a 204
semidefinite positive matrix; thus, for all i , $\lambda_i \geq 0$. It is also
205 known that $\lambda_1 = 0$ since $Le = 0$ with $e = (1, \dots, 1)$ [31]. 206

Definition: The second smallest eigenvalue $\lambda_2(L)$ is the 207
algebraic connectivity of G . 208

Now, recall the two key properties of the algebraic connec- 209
tivity that will be used in this paper. 210

Property 1: Let $e = (1, \dots, 1) \in \mathbb{R}^n$ and 211

$$\Omega = \{x \in \mathbb{R}^n \mid \|x\| = 1, \quad e^T x = 0\}.$$

The Courant–Fischer principle [32] states that 212

$$\lambda_2 = \min_{x \in \Omega} x^T L x. \quad (1)$$

Property 2: Function $w \rightarrow \lambda_2(w)$ is concave with w denot- 213
ing the edge weight vector. This can be proven by seeing that
214 $\lambda_2(w)$ is the pointwise infimum of a family of linear functions
215 of w (see [27]) 216

$$\lambda_2(w) = \inf_{\|v\|=1, e^T v=0} v^T L v,$$

$$\lambda_2(w) = \inf_{\|v\|=1, e^T v=0} \sum_{(i,j) \in E} w_{ij} (v_i - v_j)^2.$$

217 The goal of this paper is to maximize the algebraic connec-
218 tivity of the network under several constraints.

219 There are $m = (n(n-1))/2$ edges in the complete sym-
220 metric graph. Each has a weight w_{ij} representing the link
221 strength, as described in Section I. The following constraints
222 are considered.

223 The edge weight representing link strength must be within
224 the range between the lower bound α and the upper bound β

$$\forall (i, j) \in E, \quad \alpha \leq w_{ij} \leq \beta.$$

225 When there is no edge connecting v_i and v_j , the corresponding
226 $w_{ij} = 0$.

227 There exists an operating cost c_{ij} for each link. In a real air
228 transportation network, the cost for a route contains the fuel
229 cost, aircraft maintenance cost, crew/flight attendant labor cost,
230 cost for arrival/departure slots at runways, cost for gates at
231 origin/destination airports, and cost for flying through airspace
232 (international flights). In this paper, we use one link cost to
233 represent the integrated operating cost. The operating cost is
234 higher for a stronger link for several practical reasons. For
235 example, we know that the most effective way to avoid a
236 mechanical problem cancelation is to have spare parts or even
237 a spare aircraft. Similarly, the most effective way to avoid a
238 cancelation caused by crew legality or crew scheduling is to
239 have enough standby crew. Both approaches can increase link
240 strength; at the same time, they introduce higher costs. As for
241 weather disturbances, to load extra fuel will give an aircraft
242 more flight plan options with which it can be rerouted to avoid
243 weather problems and prevent the cancelation. However, extra
244 fuel also introduces higher cost. In addition, larger aircraft are
245 more robust to weather disturbances. Nevertheless, to operate
246 a larger aircraft costs more because of more fuel needed, more
247 flight attendants, and even more crew (for international flights).
248 Therefore, in this paper, we consider the linear cost for link
249 strength. The total operating cost budget for all the links is
250 limited by

$$\sum_{ij} w_{ij} c_{ij} \leq C.$$

251 In summary, the complete problem that the authors aim at
252 solving is

$$\max_w \lambda_2(L(w)) \quad \text{s.t.} \quad \begin{cases} \sum_{ij} w_{ij} c_{ij} \leq C \\ w_{ij} \in \{0, [\alpha, \beta]\} \end{cases} \quad (\text{P})$$

253 A. Alternative Formulation

254 In order to be able to solve the problem, the authors need to
255 reformulate it by adding decision variables. The idea is to add,
256 for each edge (i, j) , a binary variable x_{ij} stating if there exists
257 an edge between v_i and v_j

$$x_{ij} = 1 \Leftrightarrow w_{ij} \neq 0.$$

258 This is useful since now the domain of w can be expressed as

$$\forall (i, j), \quad \alpha x_{ij} \leq w_{ij} \leq \beta x_{ij}.$$

The problem now becomes

259

$$\max_{x, w} \lambda_2(L(w)) \quad \text{s.t.} \quad \begin{cases} x_{ij} \in \{0, 1\} \\ \sum_{ij} w_{ij} c_{ij} \leq C \\ \alpha x_{ij} \leq w_{ij} \leq \beta x_{ij} \end{cases}$$

Then, variable k is added, which determines the number of 260
edges in the graph. The final formulation of the problem is 261

$$\max_{x, w, k} \lambda_2(L(w)) \quad \text{s.t.} \quad \begin{cases} \sum_{i,j} x_{ij} = k \\ x_{ij} \in \{0, 1\} \\ \sum_{i,j} w_{ij} c_{ij} \leq C \\ \alpha x_{ij} \leq w_{ij} \leq \beta x_{ij} \end{cases} \quad (2)$$

B. Difficulty

262

An important remark is that the problem cannot really be 263
split into two steps of first deciding whether $w = 0$ or not and 264
followed by choosing the appropriate weights. This is due to 265
the fact that there are lower bound and upper bound constraints 266
on w . However, assuming that the two steps are independent, a 267
decoupled approach can be tried first. The first step is to choose 268
edges for the empty graph that corresponds to the edge addition 269
problem introduced in [25] 270

$$\begin{aligned} & \max_x \lambda_2(L(x)) \\ & \text{s.t.} : \sum_i x_i = k, \quad x_i \in \{0, 1\}, \quad \sum_i x_i c_i \leq \frac{C}{\alpha} \end{aligned}$$

and the second step is to choose the weights on them 271

$$\begin{aligned} & \max_w \lambda_2(L(w)) \\ & \text{s.t.} : \sum_i w_i c_i \leq C, \quad \alpha y_i \leq w_i \leq \beta y_i, \quad y = x_{\text{opt}}. \end{aligned}$$

Later, it will be seen that, if this approach is used, the result will 272
not be optimal. 273

C. Relaxation

274

The relaxation (R) of the problem is obtained by allowing 275
noninteger values for x 276

$$\forall (i, j) \in E, \quad x_{ij} \in [0, 1].$$

This is the same as choosing $w \in [0, \beta]$ without variables x 277
and k . However, these variables will be necessary in order to 278
be able to get the integer solution from this relaxed one. It is 279
noticed that the solution of (R) is a concave function of k . 280

D. Concavity in k

281

The first important property is that the solution of (R) is 282
concave in k , which will be used in the golden section search 283
algorithm in Algorithm 1. More precisely, Λ is defined such that 284

$$\Lambda(k) = \max_{x, w} \lambda_2(L(w)) \quad \text{s.t.} \quad \begin{cases} \sum_i x_i = k \\ x_i \in [0, 1] \\ \sum_i w_i c_i \leq C \\ \alpha x_i \leq w_i \leq \beta x_i \end{cases}$$

285 *Property 3:* $\Lambda(k)$ is a concave function.

286 This property is important since it shows that the maximiza-
287 tion of the algebraic connectivity is related to the number of
288 edges in the graph. By solving the problem for very few values
289 of k , a good knowledge on k_{opt} can be obtained.

290 *Proof:* Consider k_1 and k_2 in \mathbb{R} and $\gamma \in [0, 1]$ such that
291 $\Lambda(k_i) > 0$ for $i = 1, 2$. The idea is to use the fact that $w \rightarrow$
292 $\lambda_2(L(w))$ is concave (please see Property 2).

$$\begin{aligned} & \Lambda(\gamma k_1 + (1-\gamma)k_2) \\ &= \max_{x,w} \lambda_2 \quad \text{s.t.} \quad \begin{cases} \sum_i x_i = \gamma k_1 + (1-\gamma)k_2 \\ x_i \in [0, 1] \\ \sum_i w_i c_i \leq C \\ \alpha x_i \leq w_i \leq \beta x_i \end{cases} \\ &\geq \max_{x,w} \lambda_2 \quad \text{s.t.} \quad \begin{cases} \sum_i x_i^{(1)} = k_1, & \sum_i x_i^{(2)} = k_2 \\ x_i^{(j)} \in [0, 1], & j = 1, 2 \\ x = \gamma x^{(1)} + (1-\gamma)x^{(2)} \\ \sum_i w_i c_i \leq C \\ \alpha x_i \leq w_i \leq \beta x_i \end{cases} \\ &\geq \max_{x,w} \lambda_2 \quad \text{s.t.} \quad \begin{cases} \sum_i x_i^{(1)} = k_1, & \sum_i x_i^{(2)} = k_2 \\ x_i^{(j)} \in [0, 1], & j = 1, 2 \\ w = \gamma w^{(1)} + (1-\gamma)w^{(2)} \\ \sum_i w_i c_i \leq C \\ \alpha x_i^{(j)} \leq w_i^{(j)} \leq \beta x_i^{(j)} \end{cases} \\ &\geq \gamma \max_{x,w} \lambda_2 \quad \text{s.t.} \quad \begin{cases} \sum_i x_i = k_1 \\ x_i \in [0, 1] \\ \sum_i w_i c_i \leq C \\ \alpha x_i \leq w_i \leq \beta x_i \end{cases} \\ &\quad + (1-\gamma) \max_{x,w} \lambda_2 \quad \text{s.t.} \quad \begin{cases} \sum_i x_i = k_2 \\ x_i \in [0, 1] \\ \sum_i w_i c_i \leq C \\ \alpha x_i \leq w_i \leq \beta x_i \end{cases} \\ &\geq \gamma \Lambda(k_1) + (1-\gamma)\Lambda(k_2) \end{aligned}$$

293 which proves that Λ is concave in k . ■

294 III. SMALL-SCALE AIR TRANSPORTATION NETWORKS

295 A. Exact Solution for Small Networks

296 If all weights have to be chosen within an interval, the
297 problem becomes a convex optimization problem and it can
298 be solved using an SDP solver. The idea here is to try all the
299 possible configurations for which all the weights are either 0
300 or in $[\alpha, \beta]$. Then, each configuration can be independently
301 optimized and the one that leads to the best result can be found.

302 Consider that n nodes are chosen randomly. There are $m =$
303 $(n(n-1))/2$ edges and 2^m configurations to test. For each
304 configuration, if Y is the set of the edges that are actually in
305 the graph, the following problem needs to be solved:

$$\max_w \lambda_2(L(w)) \quad \text{s.t.} \quad \begin{cases} \sum_{i,j} w_{ij} c_{ij} \leq C \\ \alpha \leq w_{ij} \leq \beta, & \forall (i,j) \in Y \\ w_{ij} = 0, & \forall (i,j) \notin Y. \end{cases}$$

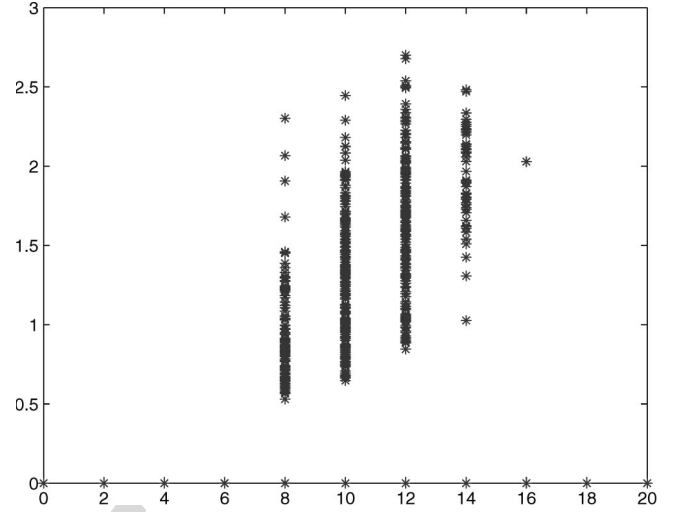


Fig. 2. Results of (k, λ_2) for all the configurations of $n = 5$ and $C = 6.5$.

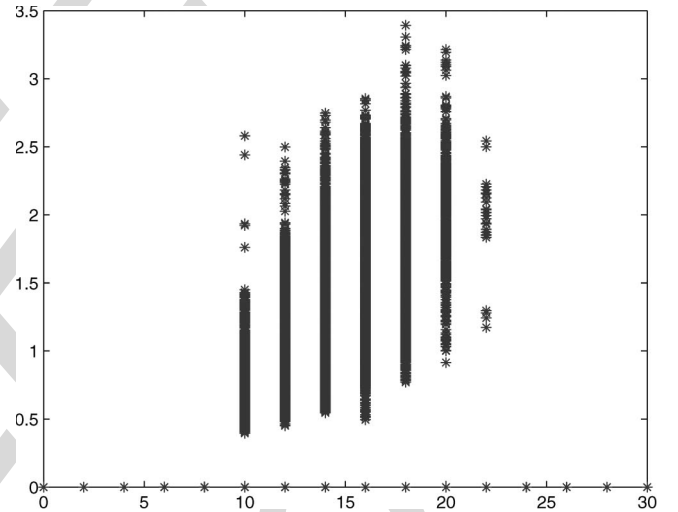


Fig. 3. Results of (k, λ_2) for all the configurations of $n = 6$ and $C = 8$.

This can be done by solving the SDP corresponding to the 306
weight optimization problem (see [27] for details) 307

$$\min_w \sum_i w_i c_i \quad \text{s.t.} \quad \begin{cases} \alpha \leq w_{ij} \leq \beta, & \forall (i,j) \in Y \\ w_{ij} = 0, & \forall (i,j) \notin Y \\ L(w) \succeq I - \frac{1}{n} ee^T. \end{cases}$$

It becomes impossible to exactly solve the problem when n is 308
large. Therefore, the authors assume n to be small in this section. 309

310 *1) Small-Scale Exact Solution Results:* For each configura-
311 tion, the number of edges k in the graph is computed. The
312 results of (k, λ_2) are plotted in Figs. 2 and 3 for two different
313 networks.

314 It is noticed that the best connectivity is not reached at the
315 maximum number of edges; therefore, the choice of the edges
316 and the choice of the weights are not independent. 316

317 It is also noticed that, unlike the continuous case, the discrete
318 shape given by $k \rightarrow \Lambda(k)$ in Figs. 2 and 3 is not exactly con-
319 cave. However, it has almost the shape of a concave function;
320 hence, the authors will be able to consider it concave in the
321 approximate case later on. 321

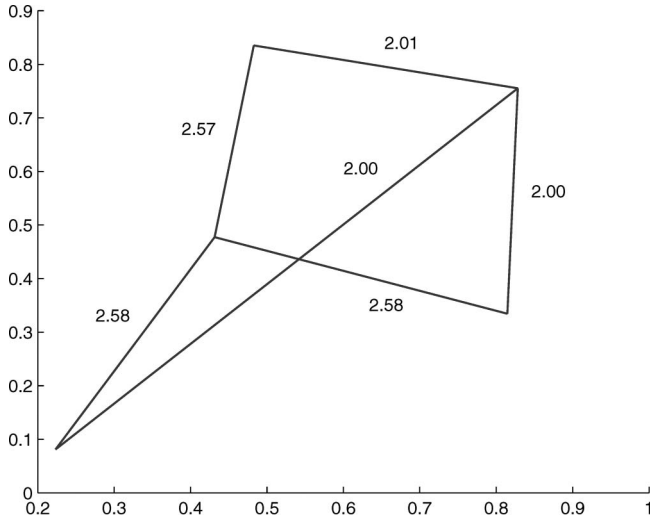


Fig. 4. Optimal network for $n = 5$ with the weights. $p = 0$, $\alpha = 2$, and $C = 6.5$.

322 The exact solution for a network of size $n = 5$ is shown
 323 in Fig. 4. As it is impossible to exactly solve this problem
 324 for networks with a larger size, an algorithm is going to be
 325 designed, which solves it approximately. The main idea is to
 326 use the quasi-concave shape of function $\Lambda(k)$.

327 For the practical problem with a larger size, the first step is to
 328 choose a value for k . The authors are able to solve the relaxed
 329 version (R) of the problem where x is a noninteger variable.
 330 Then, the result can be rounded to obtain a feasible solution for
 331 the original problem (P).

332 2) *Maximum Number of Edges*: Because of the minimum
 333 value α for the weights, there exists a limit in the number
 334 of edges in the graph. Here, the maximal number of edges
 335 k_{lim} needs to be found. Regardless of the performance of the
 336 network, edges are added until the operating cost constraint is
 337 reached. Consider that $w = \alpha x$, which is the minimum weight,
 338 and the problem is to solve a trivial form of the knapsack
 339 problem

$$\begin{aligned} & \max_{x \in \{0,1\}} \sum_i x_i \\ & \text{s.t. } \sum_i x_i c_i \leq \frac{C}{\alpha}. \end{aligned}$$

340 Indeed, if k_{lim} is the solution of this problem, it can be guaran-
 341 teed that there will not be any solution of $k > k_{\text{lim}}$.

342 When the cost c_i is sorted by increasing order, it can be
 343 obtained that

$$\sum_{s=1}^{k_{\text{lim}}} c_s \approx \frac{C}{\alpha}$$

344 which, for large-enough n , can be approximated by the follow-
 345 ing formula:

$$\int_1^{k_{\text{lim}}} g(s) ds = \frac{C}{\alpha}$$

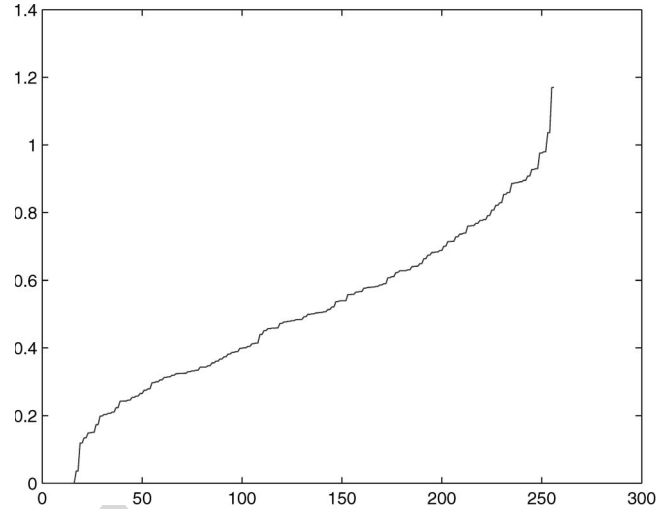


Fig. 5. Function g for random points in $[0, 1]^2$.

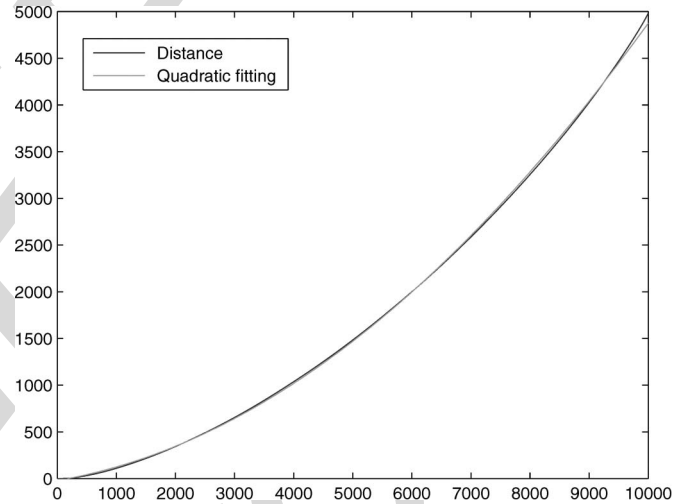


Fig. 6. C as a function of k_{lim} with the quadratic fitting.

where

$$\forall s \in [1, k_{\text{lim}}], \quad g(s) = c_{\lfloor s \rfloor}.$$

If the n nodes are randomly chosen in a square, function g 347
 348 is very close to a linear function (except at the very beginning
 349 and at the very end). This can be verified in Fig. 5. Using this
 350 information, it can be obtained that

$$a_2 k_{\text{lim}}^2 + a_1 k_{\text{lim}} + a_0 = \frac{C}{\alpha} \quad (3)$$

where a_0 , a_1 , and a_2 are constant parameters. Finally

$$k_{\text{lim}} = \frac{-a_1 + \sqrt{a_1^2 - 4a_2(a_0 - \frac{C}{\alpha})}}{2a_2}. \quad (4)$$

It is shown in Fig. 6 that the quadratic result obtained by (4) 352
 353 is a very good approximation.

354 *B. SDP Formulation*

355 To solve the larger size problem, the relaxation of the prob-
 356 lem is expressed as an SDP that will be solved efficiently. When
 357 v is not normalized, recall (1) in Property 1, which can be then
 358 transformed as

$$\begin{cases} \lambda_2 = \max_{\lambda} \lambda \\ \lambda v^T v \leq v^T L v \\ \forall v \in \mathbb{R}^n, \quad v^T e = 0. \end{cases}$$

359 Variable μ is added, which allows any $v \in \mathbb{R}^n$

$$\begin{cases} \lambda_2 = \max_{\lambda, \mu} \lambda \\ \forall v \in \mathbb{R}^n, \quad v^T (\mu e e^T) v + v^T L v - \lambda v^T v \geq 0. \end{cases}$$

360 It can be written using Loewner's order [33]

$$\begin{cases} \lambda_2 = \max_{\lambda, \mu} \lambda \\ \mu e e^T + L - \lambda I \succeq 0. \end{cases} \quad (5)$$

361 The relaxation of the problem that needs to be solved is

$$\max_{x, w, k} \lambda_2(L(w)) \quad \text{s.t.} \quad \begin{cases} \sum_i x_i = k \\ x_i \in [0, 1] \\ \sum_i w_i c_i \leq C \\ \alpha x_i \leq w_i \leq \beta x_i \end{cases}$$

362 which now becomes with (5)

$$\max_{x, w, k, \lambda, \mu} \lambda \quad \text{s.t.} \quad \begin{cases} \sum_i x_i = k \\ x_i \in [0, 1] \\ \sum_i w_i c_i \leq C \\ \alpha x_i \leq w_i \leq \beta x_i \\ \mu e e^T + L - \lambda I \succeq 0. \end{cases} \quad (6)$$

363 This problem is an SDP since there is a semidefinite constraint
 364 and all the other constraints are linear. It can be solved effi-
 365 ciently by an SDP solver. SeDuMi [34] is used in this paper.

366 1) *Optimality Conditions:* The primal SDP is

$$\max_{x, w, k, \lambda, \mu} \lambda \quad \text{s.t.} \quad \begin{cases} \sum_i x_i = k \\ x_i \in [0, 1] \\ \sum_i w_i c_i \leq C \\ \alpha x_i \leq w_i \leq \beta x_i \\ \mu e e^T + L - \lambda I \succeq 0. \end{cases}$$

367 The variables are rescaled by dividing w , k , and x by λ and C .

368 The dual SDP problem is

$$\min_{x, w, k, \lambda} \sum_i w_i c_i \quad \text{s.t.} \quad \begin{cases} \sum_i x_i = k \\ x_i \in [0, 1] \\ \alpha x_i \leq w_i \leq \beta x_i \\ L \succeq I - \frac{1}{n} J \end{cases}$$

369 where J is the all-one matrix. When x_{ij} is relaxed (please see
 370 Section II-C), the relaxed dual SDP formulation is

$$\min_{x, w, k, \lambda} \sum_i w_i c_i \quad \text{s.t.} \quad \begin{cases} 0 \leq w_i \leq \beta \\ L \succeq I - \frac{1}{n} J. \end{cases}$$

371 X is the matrix of the operating costs. The matrix format
 372 relaxed dual SDP is therefor

$$\max_X \left\langle I - \frac{1}{n} J, X \right\rangle \quad \text{s.t.} \quad \begin{cases} X \succeq 0 \\ \langle E, X \rangle = c_{ij} \end{cases}$$

373 where E is the matrix with $E_{ii} = E_{jj} = 1$ and $E_{ij} = E_{ji} = -1$.

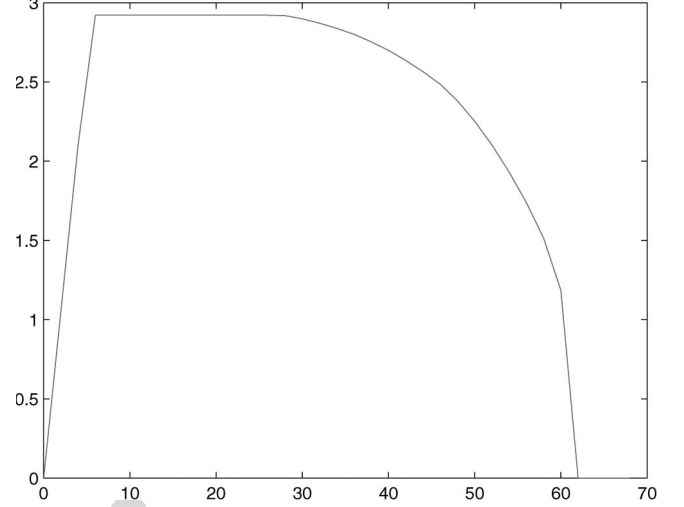


Fig. 7. Upper bound: $\lambda_2 = f(k)$.

The Karush–Kuhn–Tucker optimality conditions are

$$\begin{cases} SX = XS = 0 \\ S \succeq 0, \\ \langle E, X \rangle = c_{ij} \\ L - I + \frac{1}{n} J = S. \end{cases} \quad X \succeq 0$$

If $w_i = w$ for all i , it can be obtained that

$$S = (nw - 1) \left(I - \frac{1}{n} J \right).$$

When $w = 1/n$, $S = 0$ and the conditions are satisfied.

376 Reciprocally, if the optimality conditions are satisfied, it can
 377 be obtained that

$$\left(L - \left(I - \frac{1}{n} J \right) \right) X = 0.$$

X has rank n ; hence

$$L = I - \frac{1}{n} J.$$

Thus, w is constant for all i and $w = 1/n$.

381 For edge i and edge j , the optimality condition is finally
 382 obtained

$$\begin{cases} \forall(i, j), w_i = w_j \\ \sum_i w_i c_i = C. \end{cases}$$

2) *Upper Bound:* With the SDP formulation, the relaxation
 383 can now be solved. When the values of the optimal connectivity
 384 for different values of k are computed, the upper bound is
 385 plotted in Fig. 7.

386 The relaxed problem reached its maximum for several values
 387 of k contained in an interval $[k_{\min}, k_{\max}]$. Indeed, the optimal-
 388 ity conditions give

$$\begin{cases} \forall(i, j), w_i = w_j \\ \sum_{i=1}^m w_i c_i = C. \end{cases}$$

390 All the weights are equal and their value is $\forall i, w_i =$
 391 $(C / (\sum_j c_j)) = \Omega$. If $w = \beta x$, all the elements of x are equal

392 and their value is $\forall i, x_i = (k/(n^2 - n))$, which leads to

$$k_{\min} = \frac{\Omega(n^2 - n)}{\beta}.$$

393 By doing the same computation, it is proved that the optimal
394 value is also reached with

$$k_{\max} = \frac{\Omega(n^2 - n)}{\alpha}$$

395 and $\forall k \in [k_{\min}, k_{\max}]$, the optimal value is achieved.

396 However, it needs to be pointed out that when the solution
397 is rounded, infeasible solution may appear. For example, if $k =$
398 k_{\min} , there is often no solution since

$$\sum_i x_i = \frac{n\Omega}{\beta} < n - 1$$

399 if $(\Omega/\beta) \ll 1$, which is often the case. In addition, because at
400 least $n - 1$ edges are needed to connect an n node graph, there
401 is no positive solution. Therefore, the upper bound is not a very
402 good bound for small values of k .

403 C. Rounding Techniques for SDP Solution

404 1) *Description of the Methods:* In this section, suppose that
405 the relaxed optimal solution s_0 has been found. k edges are
406 going to be selected from s_0 , which means that $x_i = 1$ for k
407 values and $x_i = 0$ for the others. There are several ways to do
408 so. The methods that have been studied and implemented are
409 listed.

- 410 1) *Greedy:* Choose the k biggest elements $s_0(x_i)$ in the re-
411 laxed solution. Then, find the optimal weights by solving
412 the corresponding SDP.
- 413 2) *Random fast:* Randomly choose the rounding. For each
414 $i \in \{1, \dots, m\}$, $x_i = 1$ with probability $s_0(x_i)$ and $x_i =$
415 0 otherwise. Then, the weights are affected with the
416 following value:

$$\frac{s_0(w_i)}{s_0(x_i)}.$$

417 These two steps are repeated many times. The average
418 value $\overline{x_i}$ of x_i is $s_0(x_i)$; therefore

$$\overline{\sum_i x_i} = \sum_i s_0(x_i) = k$$

419 and for the same reason

$$\overline{\sum_i w_i c_i} = \sum_i \frac{s_0(w_i)}{s_0(x_i)} \overline{x_i} c_i = \sum_i s_0(w_i) c_i \leq C.$$

420 Thus, on average, the solution satisfies the constraints.
421 At the end, keep the best solution that satisfies all the
422 constraints.

- 423 3) *Random:* In addition, randomly choose the rounding. If
424 $\sum_i x_i = k$, which is the case on average, evaluate the
425 weights by solving the SDP formulation. The steps are
426 repeated several times, and keep the best value.

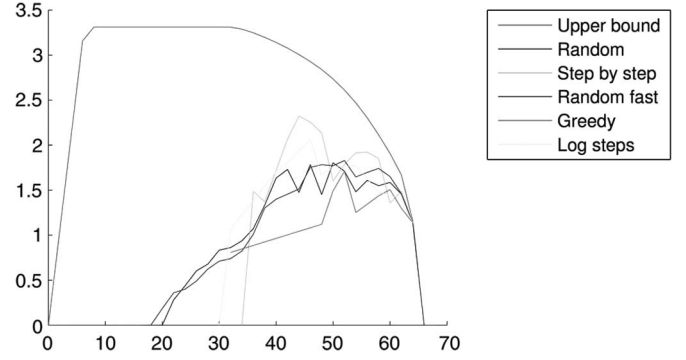


Fig. 8. λ_2 as a function of k . The results from several rounding methods are represented for a 20-node graph.

- 4) *Step by step:* Select the biggest element $s_0(x_i) < 1$ and
427 affect its value to 1 in the SDP formulation. Then, solve
428 the SDP again and repeat k times for these two steps. 429
- 5) *Log step by step:* This is the same idea as the “step by
430 step” except that, at each step, choose the best half of
431 the remaining elements. Thus, there are only $\log(k)$ SDPs
432 that have to be solved. 433

2) *Numerical Results:* The simulation is set up with 20
434 nodes randomly generated in a square. The results are presented
435 in Fig. 8 with λ_2 as a function of k . The upper bound ob-
436 tained by the relaxation is plotted, as well as all the rounding
437 techniques. 438

It turns out that some techniques may fail to find a solution. In
439 this case, the corresponding values are removed from the figure. 440

It can be seen that the algorithms can achieve the upper
441 bound at the maximum number of edges k_{\lim} . This shows that
442 any algorithm based on edge addition without considering the
443 variable weights is not adapted. 444

Pros and Cons: Each of the methods presented has some
445 advantages and drawbacks. The one that gives the best result is
446 the *step-by-step* method. The fastest is *random fast*. In addition,
447 the method that gives the best tradeoff between speed and value
448 is *log step by step*. 449

450 D. Relaxed SDP With Rounding Algorithm

This algorithm is used to solve relatively small-scale problem
451 when the exhaustive search described in Section III-A fails. 452

- 1) *Golden Section Search:* For a given k , a well-connected
453 network with k edges can now be found. Instead of testing all
454 the possible values of k , the search can be speeded up by con-
455 sidering that algebraic connectivity is a concave function of k . 456

This approximation leads to better results with rounding
457 methods that have good regularity. For large networks, the
458 rounding methods with lower regularity can be used. Instead
459 of computing the value for a given k , a local average value is
460 computed based on three values 461

$$\forall k \in \mathbb{N}, \quad \tilde{f}(k) = \frac{f(k-1) + f(k) + f(k+1)}{3}.$$

As only the value of the connectivity for integer values
462 of k can be computed, it is not possible to use continuous
463 optimization principles. Thus, the golden section search [35] 464

465 is adopted. It consists in creating a decreasing set of intervals
466 containing the optimal value

$$\forall i \in \mathbb{N}, \quad [a_{i+1}, b_{i+1}] \subset [a_i, b_i]$$

467 and $k_{\text{opt}} \in [a_i, b_i]$. Two test values $c_i < d_i$ in $[a_i, b_i]$ facilitate
468 the search. The rules used to update the interval are: 1) $f(c_i) <$
469 $f(d_i) \Rightarrow [a_{i+1}, b_{i+1}] = [c_i, b_i]$ and 2) $f(c_i) > f(d_i) \Rightarrow$
470 $[a_{i+1}, b_{i+1}] = [a_i, d_i]$.

471 At each step, only one new value of f needs to be computed.
472 This new value is usually chosen so that the test values are at
473 the golden ratio $\phi = (1 + \sqrt{5})/2$. Here, the value is rounded
474 to get an integer. This method allows, on average, to divide the
475 length of the interval by ϕ at each step.

476 2) *Relaxed SDP With Rounding Algorithm*: All the steps
477 of the algorithm are summed up. The SDP is solved using
478 the SeDuMi solver [34] and the golden section search. This
479 algorithm that leads to the approximation of the optimum is
480 listed in Algorithm 1.

481 Algorithm 1 Relaxed SDP with step-by-step rounding

```

482 1: Initialize  $a, b$  and  $d$ 
483 2: while  $b - a > 2$  do
484 3:   Choose  $c$  in  $\{(a + d/2), (d + b/2)\}$ 
485 4:   Solve the relaxed SDP with  $k = c$ 
486 5:   for  $p = 1$  to  $k$  do
487 6:      $j \leftarrow \arg \max_i \{x_i | x_i < 1\}$ 
488 7:     Impose  $x_j = 1$ 
489 8:     Solve the SDP
490 9:   end for
491 10:  if  $f(c) < f(d)$  then
492 11:     $a \leftarrow c$ 
493 12:  else
494 13:     $b \leftarrow d, d \leftarrow c$ 
495 14:  end if
496 15: end while
497 16: return  $\lambda_2$ 

```

498 The complexity of this algorithm can be analyzed, which
499 depends on several parameters of the problem. The algorithm
500 uses the step-by-step rounding technique and requires to solve
501 $k + 1$ SDPs for each value of k selected. Each step has a
502 different value for k , and most of them are close to k_{opt} .
503 In addition, there are U such steps. U is defined by
504 $k_{\text{lim}} \phi^{-U} = 1$ since at each step the length of the interval is
505 divided by ϕ . It is obtained that

$$U = \frac{\log(1/k_{\text{lim}})}{\log(1/\phi)}.$$

506 Complexity T also needs to be considered to solve the SDP.
507 T is a polynomial in the size of the entry, which is equivalent to
508 n^2 . Therefore, T is a polynomial function of n .

509 Therefore, the complexity of the whole algorithm can be
510 approximated by $O(k_{\text{opt}} UT)$.

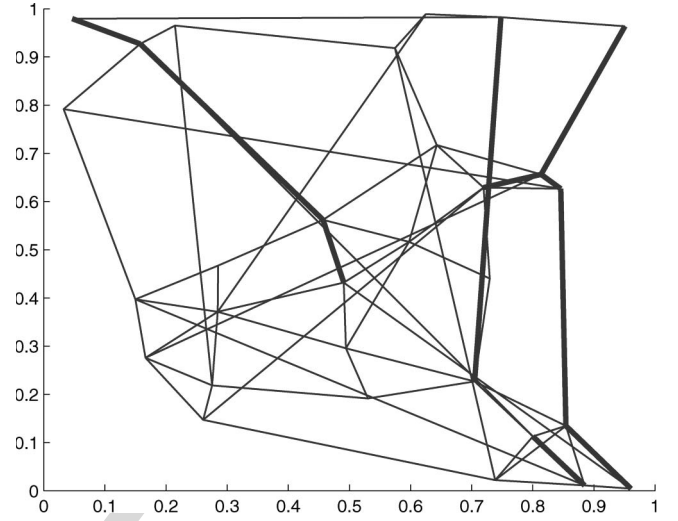


Fig. 9. Optimal result for a 30-node graph.

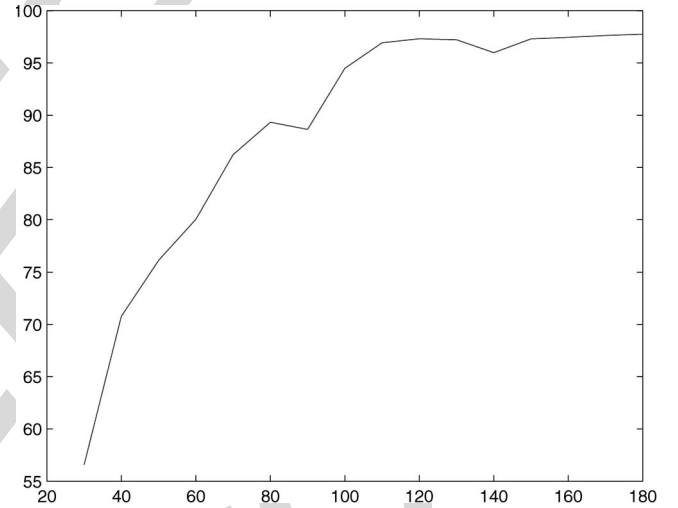


Fig. 10. Values of r for different values of C .

E. Numerical Results

511

512 1) *Optimal Network*: In order to test the full algorithm, a 512
513 set of random nodes is generated in a square. An example of
514 the optimal network for 30 nodes is shown in Fig. 9.

515 The edges that have a weight greater than the lower bound
516 α are represented with a thicker line. In the example in Fig. 9,
517 there are ten edges with a larger weight value than α .

518 2) *Efficiency*: Now, the efficiency of the result is going to
519 be evaluated by comparing the optimal algebraic connectivity
520 to the upper bound. For a given set of nodes, the problem is
521 solved for different values of the total operating cost budget C
522 and the percentage of the solution is computed compared to the
523 bound

$$r = 100 \times \frac{\text{val}(P)}{\text{val}(R)} \%$$

524 The result, as illustrated in Fig. 10, shows that for small
525 values of C , the best result found is very far from the upper

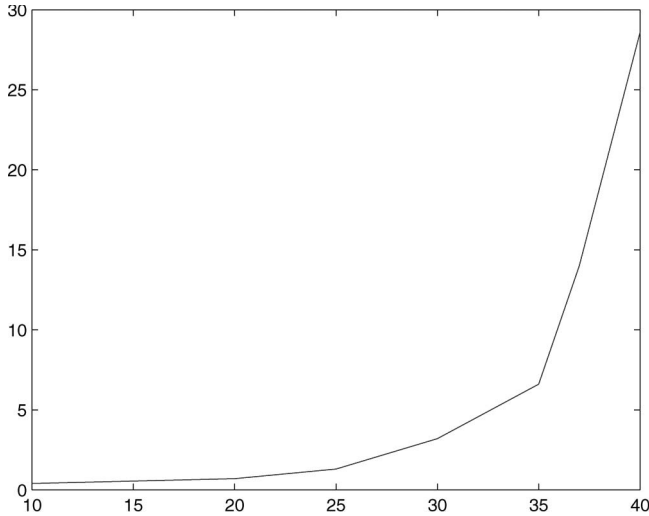


Fig. 11. Time (in seconds) to solve the SDP formulation of the problem for a given number of n nodes.

526 bound. However, when increasing C , the objective value of the
527 problem P quickly increases to reach the value of its relaxed
528 problem R .

529 IV. LARGE-SCALE AIR TRANSPORTATION NETWORKS

530 A. Necessity

531 The method in the previous section is going to be applied to
532 large networks. The most time-consuming computation in the
533 process is solving the SDP. Fig. 11 shows the computational
534 time of solving one SDP for n nodes. It is observed that the
535 running time increases very rapidly. In fact, for n nodes, there
536 are $n(n-1) + 2 \sim n^2$ variables in the SDP. As several SDPs
537 need to be computed in order to solve the problem, it becomes
538 impossible for $n \geq 35$ on the authors' workstation.

539 However, it is necessary to get some results for large values
540 of n because real networks are usually large. For example, the
541 air transportation network contains several hundred nodes when
542 considering the entire USA.

543 B. Cluster Decomposition

544 Since the key factor for operating cost for each link is the
545 route distance (a longer distance route consumes more fuel), the
546 idea in this section is to divide the airports into $g \in \mathbb{N}$ clusters
547 based on the distance between the nodes. These clusters can be
548 solved independently with the relaxed SDP method (Algorithm 1)
549 developed in the previous section and can be connected
550 afterward.

551 To connect the cluster, choose k major nodes in each cluster
552 that will be connected to each other. Then, the problem P has to
553 be solved for these $g \times k$ nodes, except that links between two
554 nodes from the same cluster are not allowed; hence, the graph
555 is not complete.

556 At the end, $g+1$ problems of type (P) need to be solved to
557 get the final result. Fig. 12 shows the idea of the decomposition
558 into several clusters and the selection of major nodes.

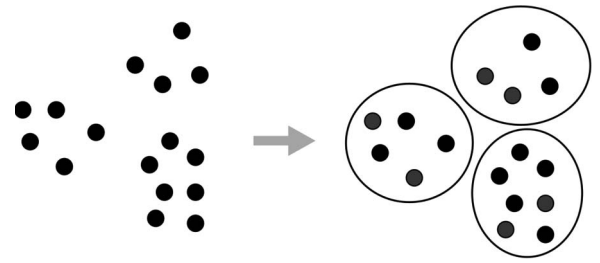


Fig. 12. Set of 16 nodes separated in three clusters with two major nodes in each cluster (in red).

There are several parameters whose values have to be chosen
559 to apply this idea. First, choose the number of clusters and how
560 many major nodes are used in each cluster to connect to other
561 clusters. Second, choose which nodes are kept as major nodes
562 among each cluster. Naturally, it is decided here to take the
563 airports that have the largest traffic demand. 564

In addition, to solve the problem for each small problem $1 \leq$
565 $i \leq g+1$, the value of the maximum operating cost budget C_i
566 in each cluster has to be chosen. A natural option is to choose
567 C_i proportional to the sum s_i of all the costs of the edges in the
568 cluster i and such that $\sum_{i=1}^{g+1} C_i = C$ 569

$$s_i = \sum_{(x,y) \in E} c_{xy},$$

$$C_i = \frac{s_i}{\sum_{j=1}^{g+1} s_j} C.$$

The separation of the nodes into several clusters is made
570 by k -means algorithm [36]. This algorithm has the advantages
571 of being fast, easy to implement, and generally giving good
572 results. 573

To sum up the method described above, the full cluster
574 decomposition algorithm is listed in Algorithm 2. 575

Algorithm 2 Large-scale cluster decomposition

- | | |
|---|-----|
| 1: Initialize g, C_i | 577 |
| 2: k -means algorithm gives g clusters | 578 |
| 3: for $p = 1$ to g do | 579 |
| 4: Solve the cluster problem (with Algorithm 1) | 580 |
| 5: end for | 581 |
| 6: Solve the major node problem (Algorithm 1) | 582 |
| 7: Build the resulting network | 583 |
| 8: return $\lambda_2(L)$ | 584 |
-

C. Evaluation of Efficiency

The goal here is to show that if all $g+1$ clusters are well
586 connected, the resulting graph is well connected too. This
587 depends on the values of some parameters that characterize how
588 each cluster is linked to the others. 589

g clusters are considered. Each cluster has n nodes and k
590 of its nodes are used to connect to other clusters. Let G be
591 the matrix of the graph and F be the vector defined by the
592

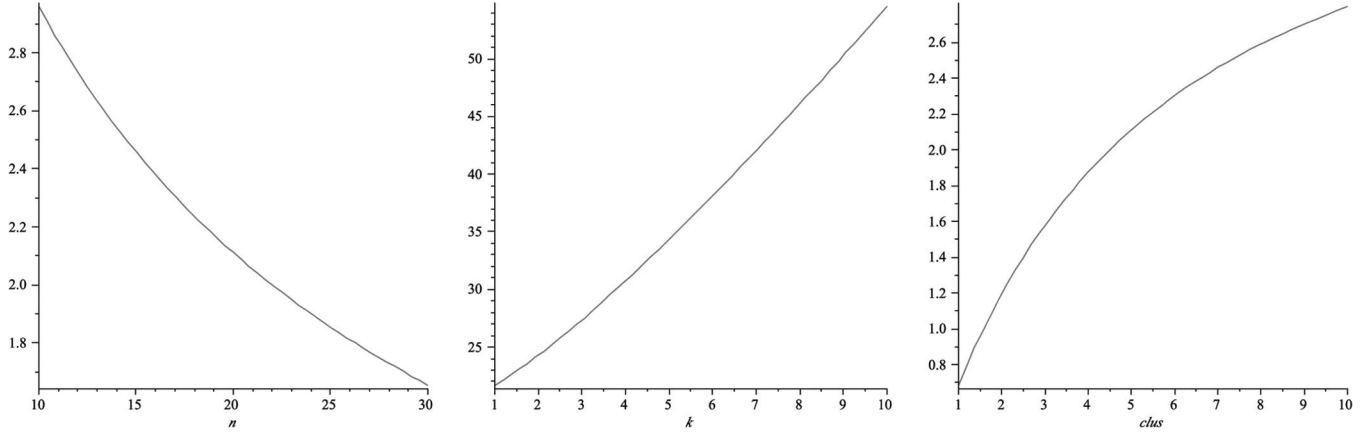


Fig. 13. (a) $\lambda_2 = f(n)$; (b) $\lambda_2 = f(k)$; (c) $\lambda_2 = f(g)$.

593 expression below. If, for instance, $g = 3$, matrix G can be put
594 into the following form:

$$G = \begin{pmatrix} & & & E & 0 & 0 & E & 0 & 0 \\ & A_1 & & 0 & 0 & 0 & 0 & 0 & 0 \\ & & & 0 & 0 & 0 & 0 & 0 & 0 \\ E & 0 & 0 & & & & E & 0 & 0 \\ 0 & 0 & 0 & & A_2 & & 0 & 0 & 0 \\ 0 & 0 & 0 & & & & 0 & 0 & 0 \\ E & 0 & 0 & E & 0 & 0 & & & \\ 0 & 0 & 0 & 0 & 0 & 0 & & A_3 & \\ 0 & 0 & 0 & 0 & 0 & 0 & & & \end{pmatrix}$$

$$F = \begin{pmatrix} \alpha e \\ \beta e \\ \frac{\beta e}{0} \\ 0 \\ \frac{0}{-\alpha e} \\ -\beta e \\ -\beta e \end{pmatrix}$$

595 with the following notation. e is the all-one vector. α and β are
596 constants that will be computed in the next paragraph. A_1 , A_2 ,
597 and A_3 represent the adjacency matrices of the three clusters.
598 E is a $k \times k$ matrix with all elements equal to 1.

599 1) *Fiedler Vector*: The Fiedler vector is the vector solution
600 of the minimization problem

$$\min_{x \in \mathbb{R}^n} \{x^T Lx \mid \|x\| = 1, \quad xe = 0\}.$$

601 It is known to be an indicator on how to split a graph into two
602 smaller graphs. In fact, the nodes that have the same sign in this
603 vector form a cut of the graph (see [37]).

604 Here, the optimal cut will naturally be found between two
605 clusters. Since some of the nodes play the same role, the Fiedler
606 vector has a shape close to F where α and β are constants that
607 need to be determined.

608 This assumption has been verified by numerical experiments
609 and it seems to be a very good approximation of the real Fiedler
610 vector.

611 2) *Computing the Connectivity*: Consider that the Fiedler
612 vector has the form of F and matrices are full, which means

all nondiagonal elements are equal to 1. The matrix products
613 give
614

$$\lambda_2 = F^T L F,$$

$$\lambda_2 = 2k\alpha X + 2(n-k)\beta Y$$

with

$$X = \alpha(n-1+k(g-1)) - (k-1)\alpha - (n-k)\beta + k\alpha,$$

$$Y = \beta(n-1) - k\alpha - (n-k-1)\beta.$$

It is also known that $\|F\| = 1$; thus

$$2k\alpha^2 + (2n-2k)\beta^2 = 1,$$

$$\alpha = \sqrt{\frac{1 - (2n-2k)\beta^2}{2k}}.$$

Substitute α with this expression and β is given by the

$$\frac{d\lambda_2}{d\beta} = 0. \tag{7}$$

615 With a computation software package like Maple, this gives
616
617
618
619

$$\lambda_2 = f(n, k, g).$$

3) *Resulted Curves*: By solving (7), the values of α , β , and
620 λ_2 are obtained. The following figures have been obtained with
621 Maple. Among the three parameters k , g , and n , fix two of them
622 and let the third one vary to see its influence on connectivity.
623

Fig. 13 provides a clearer idea on how to choose the value
624 of each parameter. For example, connectivity is almost linear
625 regarding k but has a concave shape when represented as a
626 function of the number of clusters g .
627

There exists a tradeoff: If g is too large, kg will be too large to
628 be solved. On the contrary, if g is too small, each of the cluster
629 will have too many nodes to be solved.
630

4) *Numerical Results*: The data used are the 100 largest
631 cities in the United States. Fig. 14 shows the 100 biggest
632 cities without any link. The cluster decomposition is used to
633 divide these 100 cities into $g = 5$ groups. In each group, we
634 selected $k = 5$. The lower bound $\alpha = 2$ and the upper bound
635

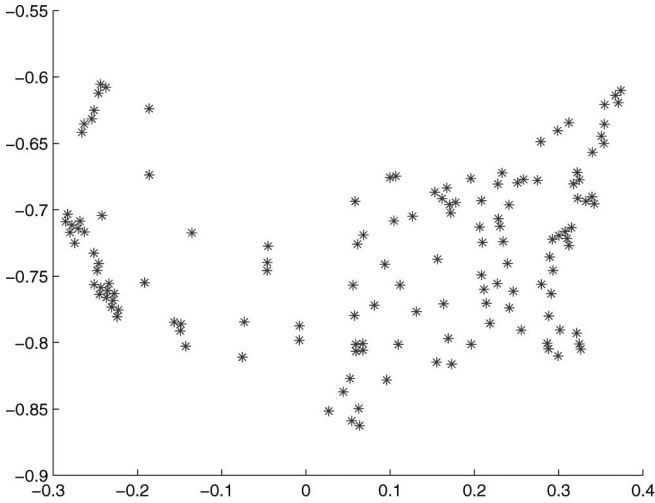


Fig. 14. Shown are the 100 largest cities in the USA.

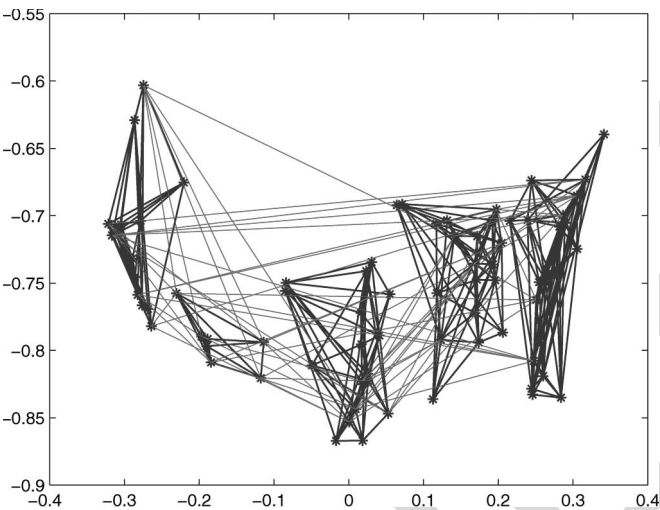


Fig. 15. Result for the 100 largest cities in the USA.

636 $\beta = 10$. The total running time is 317 s with MATLAB on our
637 workstation. The algebraic connectivity that we have achieved
638 is $\lambda_2 = 2.6$.

639 The optimal network found is illustrated in Fig. 15. The blue
640 lines represent the edges inside each cluster and the red lines
641 represent the edges that connect nodes from different clusters.

642 In a real network, most airlines use spoke-hub planning, in
643 which the regional airports are clustered and connected to their
644 regional hub airport. Fig. 15 shows the same behavior that
645 regional airports are clustered together. In a real network in the
646 United States, the number of the major nodes k for each cluster
647 is usually 1, which means that the hub airport is the only major
648 node for its cluster. In a real network in Europe, the number of
649 the major nodes k is usually bigger than 1. In fact, the number
650 k in a European network is those hub airports in each country.
651 For example, Air France has hubs at Paris and Lyon ($k = 2$)
652 and Air Berlin has its hubs at Berlin, Düsseldorf, Hamburg, and
653 Munich ($k = 4$). In summary, the result in Fig. 15 is a practical
654 design, and more importantly, the computation is very efficient
655 for large-scale network planning.

V. DIRECTED AIR TRANSPORTATION NETWORK 656

A. From Undirected Graph to Directed Graph 657

In this section, the methods are extended in directed graphs. 658
In order to be consistent with the undirected case, the graphs 659
need to be balanced, which means that the number of aircraft 660
that comes in is the same as the number of aircraft that leaves 661
the airport 662

$$\forall i \in \{1, \dots, n\}, \quad \sum_{j=1}^n w_{ij} = \sum_{k=1}^n w_{ki}.$$

It is clear that the set of undirected graphs is included in the set 663
of directed balanced graphs. Therefore, the results should be at 664
least as good as in the previous section. 665

Definition: According to [38], if $\Omega = \{x \in \mathbb{R}^n, xe = 666$
 $0, \|x\| = 1\}$, the definition of the algebraic connectivity can be 667
extended for directed balanced graphs with 668

$$\min_{x \in \Omega} x^T L x = \lambda_2 \left(\frac{1}{2} (L + L^T) \right).$$

Property 4: In the directed case and with this definition 669
of the algebraic connectivity, the upper bound given by the 670
continuous relaxation is the same as in the undirected case. 671

Proof: Given the optimum directed balanced graph in the 672
relaxed problem and its incidence matrix G , H can be created 673

$$H = \frac{G + G^T}{2}$$

where H is symmetric and satisfies all the constraints of the 674
problem since they are linear. In addition with the definition of 675
the connectivity for directed graphs, the connectivity of H is 676
clearly the same as the connectivity of G . 677

Since it is also known that undirected graphs are a subset of 678
directed balanced graphs, the bounds are equal in both cases. 679
This will allow us to easily evaluate the improvement brought 680
by directed graphs. ■ 681

B. Results 682

The same method is used as in Section III. The results are 683
impressively better with directed graphs, as shown in Fig. 16. 684
The best value for the directed balanced case almost reached 685
the upper bound. It is also noticed that the optimal result has 686
less edges than the optimal network in the undirected case (an 687
edge in the undirected case is counted in both ways). 688

It is shown in Fig. 17 that most of the edges in the optimal 689
solution are oriented in only one way, which shows that the 690
solution is very different from the undirected case. 691

However, there is an important drawback. Indeed, two times 692
as many variables are needed for directed networks. Thus, the 693
problem takes a much longer time to be solved and is only 694
applicable on smaller networks. 695

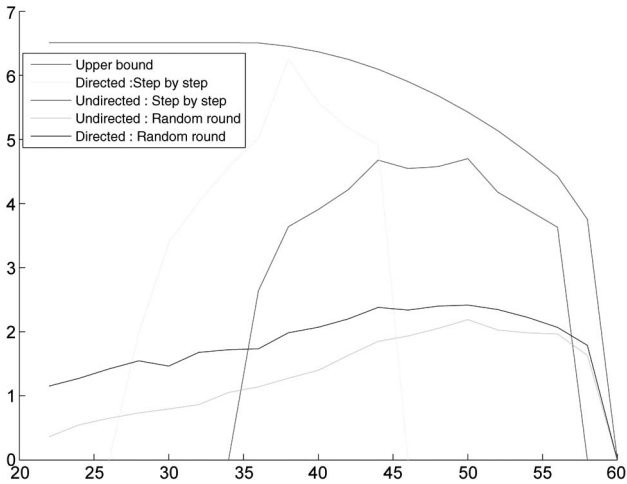


Fig. 16. $\lambda = f(k)$ for the same graph with different approaches.

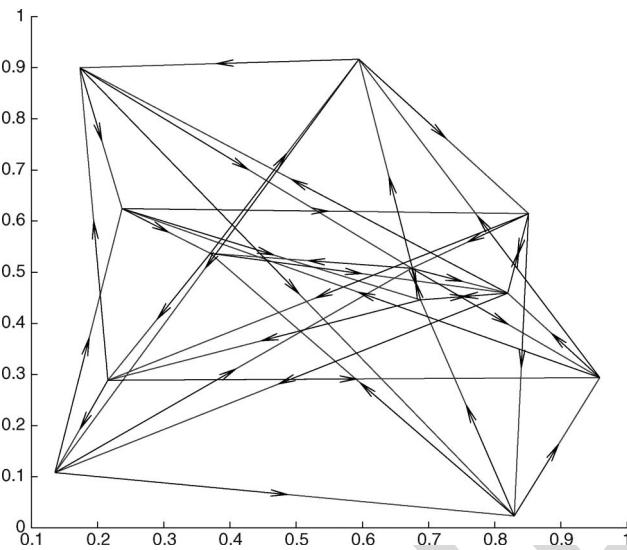


Fig. 17. Optimal directed graph.

696 C. Failure Case

697 If an edge or a node is removed, the graph is not balanced
698 anymore. This can cause important problems in practice; hence,
699 the remaining weights in the graph need to be changed to handle
700 this problem.

701 This operation can be done by using a flow algorithm. The
702 first step is to link the nodes with positive aircraft balance to a
703 virtual source and those with negative balance to a sink. The ca-
704 pacities of these links are equal to the absolute value of the
705 difference in the balance flow for the node. The capacity of the
706 other links of the graph is β .

707 Then, consider the problem of the maximization of the flow
708 from the source to the sink. This problem can be solved by using
709 Edmonds–Karp algorithm [39], which has efficient complexity,
710 i.e., $O(nm^2)$. This algorithm maintains the balance of the flow
711 at each node.

712 At the end, the graph is the graph solution of the flow
713 problem when the source and the sink are removed. Figs. 18
714 and 19 show an example of a graph in which a node is removed,

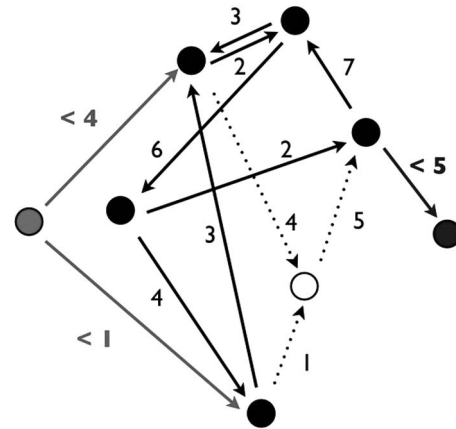


Fig. 18. Example of a graph with a node failure.

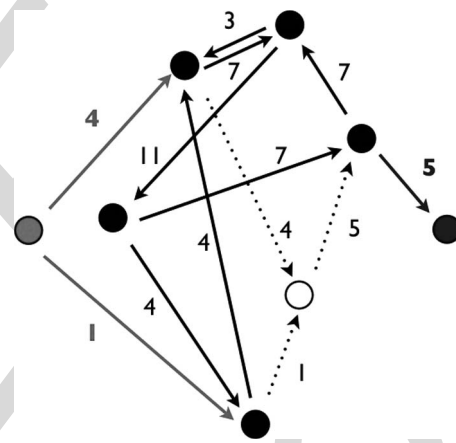


Fig. 19. Example of a graph after maximization of the flow.

before and after maximization of the flow. The graph in Fig. 19
715 is now balanced by Edmonds–Karp algorithm after removing 716
the source (green node) and the sink (blue node). 717

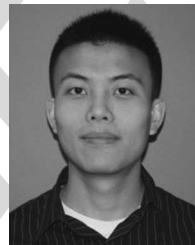
VI. CONCLUSION

In this paper, a new problem concerning the maximization of
719 the algebraic connectivity of a network has been presented and
720 studied. This problem consists of finding both the edges of the
721 graph and their weight assignment under several constraints. 722
First, the problem in small networks is exactly solved, and it is
723 shown that the problem cannot be separated into two already
724 studied independent problems. Then, a relaxed SDP method
725 with step-by-step rounding is presented to solve the problem
726 approximately for better computational efficiency. With the
727 method developed for small-scale network, the cluster decom-
728 position method is proposed to solve the large-scale network
729 problem and successfully find the near-optimal solution for a 730
network of the 100 largest cities in the United States. Finally,
731 the study is extended to directed graphs. Numerical experiments
732 and analysis are performed for all the proposed algorithms. The
733 developed methods are able to model and maximize robustness
734 in air transportation networks for airlines and for the NAS. They
735 also provide an option to improve current ways of the generic
736 network design. 737

738

REFERENCES

- [1] R. Guimera and L. Amaral, "Modeling the world-wide airport network," *Eur. Phys. J. B, Condens. Matter Complex Syst.*, vol. 38, no. 2, pp. 381–385, Mar. 2004.
- [2] R. Kincaid, N. Alexandrov, and M. Holroyd, "An investigation of synchrony in transport networks," *Complexity*, vol. 14, no. 4, pp. 34–43, Mar./Apr. 2008.
- [3] E. Vargo, R. Kincaid, and N. Alexandrov, "Towards optimal transport networks," *J. Syst., Cybern. Inf.*, vol. 8, no. 4, pp. 59–64, Jul. 2010.
- [4] International Civil Aviation Organization (ICAO), "Procedures for air navigation services—Rules of the air and air traffic services," Montréal, QC, Canada, doc 4444-RAC/501, 2010.
- [5] P. Kostiuk, D. Lee, and D. Long, "Closed loop forecasting of air traffic demand and delay," presented at the 3rd USA/Europe Air Traffic Management R&D Seminar, Napoli, Italy, Jun. 2010, Paper 80.
- [6] K. Nam and T. Schaefer, "Forecasting international airline passenger traffic using neural networks," *Logist. Transp. Rev.*, vol. 31, no. 3, pp. 239–251, Sep. 1995.
- [7] F. Alamdari and S. Fagan, "Impact of the adherence to the original low cost model on the profitability of low cost airlines," *Transp. Rev.*, vol. 25, no. 3, pp. 377–392, May 2005.
- [8] M. Dresner, J.-S. C. Lin, and R. Windle, "The impact of low-cost carriers on airport and route competition," *J. Transp. Econ. Policy*, vol. 30, no. 3, pp. 309–328, Sep. 1996.
- [9] K. Button and S. Lall, "The economics of being an airport hub city," *Res. Transp. Econ.*, vol. 5, pp. 75–105, 1999.
- [10] T. Oum, A. Zhang, and Y. Zhang, "A note on optimal airport pricing in a hub-and-spoke system," *Transp. Res. B, Methodol.*, vol. 30, no. 1, pp. 11–18, Feb. 1996.
- [11] X.-B. Hu, W.-H. Chen, and E. Di Paolo, "Multi-airport capacity management: Genetic algorithm with receding horizon," *IEEE Trans. Intell. Transp. Syst.*, vol. 8, no. 2, pp. 254–263, Jun. 2007.
- [12] X.-B. Hu and E. Di Paolo, "Binary-representation-based genetic algorithm for aircraft arrival sequencing and scheduling," *IEEE Trans. Intell. Transp. Syst.*, vol. 9, no. 2, pp. 301–310, Jun. 2008.
- [13] Y. Eun, I. Hwang, and H. Bang, "Optimal arrival flight sequencing and scheduling using discrete airborne delays," *IEEE Trans. Intell. Transp. Syst.*, vol. 11, no. 2, pp. 359–373, Jun. 2010.
- [14] Z.-H. Zhan, J. Zhang, Y. Li, O. Liu, S. Kwok, W. Ip, and O. Kaynak, "An efficient ant colony system based on receding horizon control for the aircraft arrival sequencing and scheduling problem," *IEEE Trans. Intell. Transp. Syst.*, vol. 11, no. 2, pp. 399–412, Jun. 2010.
- [15] *FlightStats-Global Flight Tracker, Status Tracking and Airport Information*, FlightStats, Inc., Portland, OR, USA, 2013, retrieved on March 16, 2013. [Online]. Available: <http://www.flightstats.com>
- [16] Federal Aviation Administration (FAA), "FAA Aerospace Forecasts FY 2008–2025," Washington, DC, USA, Dec. 2010.
- [17] S. Conway, "Scale-free networks and commercial air carrier transportation in the United States," in *Proc. 24th Int. Congr. Aeron. Sci.*, Yokohama, Japan, 2004, pp. 1–12.
- [18] P. A. Bonnefoy, "Scalability of the air transportation system and development of multi-airport systems: A worldwide perspective," Ph.D. dissertation, MIT, Cambridge, MA, USA, Jun. 2008.
- [19] N. Alexandrov, "Transportation network topologies," NASA Langley Res. Center, Hampton, VA, USA, Tech. Rep., 2004.
- [20] T. Kotegawa, D. DeLaurentis, K. Noonan, and J. Post, "Impact of commercial airline network evolution on the US air transportation system," in *Proc. 9th USA/Europe ATM Res. Develop. Semin.*, Berlin, Germany, 2011.
- [21] A. Bigdeli, A. Tizghadam, and A. Leon-Garcia, "Comparison of network criticality, algebraic connectivity, and other graph metrics," presented at the 1st Annu. Workshop Simplifying Complex Network Practitioners, Venice, Italy, 2009, Paper 4.
- [22] A. Jamakovic and S. Uhlig, "On the relationship between the algebraic connectivity and graph's robustness to node and link failures," in *Proc. 3rd EuroNGI Netw. Conf.*, May 2007, pp. 96–102.
- [23] A. Jamakovic and P. V. Mieghem, "On the robustness of complex networks by using the algebraic connectivity," in *Proc. Netw. Ad Hoc Sensor Netw., Wireless Netw., Next Gen. Internet*, A. Das, H. K. Pung, F. Bu Sung Lee, and L. Wong Wai Choong, Eds., 2008, pp. 183–194.
- [24] R. H. Byrne, J. T. Feddema, and C. T. Abdallah, "Algebraic connectivity and graph robustness," Sandia Nat. Lab., Albuquerque, NM, USA, Tech. Rep., Jul. 2009.
- [25] P. Wei and D. Sun, "Weighted algebraic connectivity: An application to airport transportation network," in *Proc. 18th IFAC World Congress*, Milan, Italy, Aug. 2011, pp. 13 864–13 869.
- [26] A. Ghosh and S. Boyd, "Growing well-connected graphs," in *Proc. 45th IEEE Conf. Decis. Control*, Dec. 2006, pp. 6605–6611.
- [27] J. Sun, S. Boyd, L. Xiao, and P. Diaconis, "The fastest mixing Markov process on a graph and a connection to a maximum variance unfolding problem," *SIAM Rev.*, vol. 48, no. 4, pp. 681–699, Nov. 2006.
- [28] F. Goring, C. Helmsberg, and M. Wappler, "Embedded in the shadow of the separator," *SIAM J. Optim.*, vol. 19, no. 1, pp. 472–501, Feb. 2008.
- [29] S. Boyd, "Convex optimization of graph Laplacian eigenvalues," in *Proc. Int. Congr. Math.*, 2006, vol. 3, pp. 1311–1319.
- [30] S. Boyd, P. Diaconis, and L. Xiao, "Fastest mixing Markov chain on a graph," *SIAM Rev.*, vol. 46, no. 4, pp. 667–689, Dec. 2004.
- [31] M. Fiedler, "Algebraic connectivity of graphs," *Czechoslovak Math. J.*, vol. 23, no. 98, pp. 298–305, 1973.
- [32] B. Mohar, "The Laplacian spectrum of graphs," in *Graph Theory, Combinatorics, and Applications*. New York, NY, USA: Wiley, 1991, pp. 871–898.
- [33] M. Siotani, "Some applications of Loewner's ordering on symmetric matrices," *Ann. Inst. Stat. Math.*, vol. 19, no. 1, pp. 245–259, Dec. 1967.
- [34] J. F. Sturm, "Using SeDuMi 1.02, A Matlab toolbox for optimization over symmetric cones," *Optim. Methods Softw.*, vol. 11, no. 1–4, pp. 625–653, Jan. 1999.
- [35] W. Press, S. Teukolsky, W. Vetterling, and B. Flannery, *The Art of Scientific Computing*, 3rd ed. Cambridge, U.K.: Cambridge Univ. Press, 2007, ch. Section 10.2. Golden Section Search in One Dimension, pp. 492–496.
- [36] J. Kleinberg and E. Tardos, *Algorithm Design*. Reading, MA, USA: Addison-Wesley, 2005, ch. 4.7 Clustering, pp. 157–161.
- [37] S. Martinez, G. Chatterji, D. Sun, and A. Bayen, "A weighted graph approach for dynamic airspace configuration," presented at the AIAA Conf. Guidance, Control Dynamics, Hilton Head, SC, USA, Aug. 2007, Paper AIAA 2007-6448.
- [38] C. Wu, "Algebraic connectivity of directed graphs," *Linear Multilinear Algebra*, vol. 53, no. 3, pp. 203–223, Jun. 2005.
- [39] T. H. Cormen, C. E. Leiserson, R. L. Rivest, and C. Stein, *Introduction to Algorithms*. Cambridge, MA, USA: MIT Press, 2009, ch. 26.2 The Ford-Fulkerson method, pp. 727–730.



Peng Wei (M'12) received the Bachelor's degree in automation from Tsinghua University, Beijing, China; the Master's degree in electrical engineering from Stony Brook University, Stony Brook, NY, USA; and the Ph.D. degree in aerospace engineering from Purdue University, West Lafayette, IN, USA.

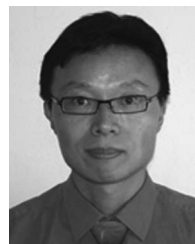
He is an Operations Research Consultant with American Airlines, Fort Worth, TX, USA. His research interests include next-generation air transportation system, environmental impact of aviation and unmanned aerial vehicle integration in the National Airspace System.

Dr. Wei received the Purdue College of Engineering Outstanding Research Award in 2013.



Gregoire Spiers received the Bachelor's degree in applied mathematics from École Polytechnique, Palaiseau, France, in 2012.

He was a Visiting Student with Purdue University, West Lafayette, IN, USA, in 2011. He is currently a Research Engineer with Amadeus S.A.S., Sophia Antipolis, France.



Dengfeng Sun (M'08) received the Bachelor's degree in precision instruments and mechatronics from Tsinghua University, Beijing, China; the Master's degree in industrial and systems engineering from The Ohio State University, Columbus, OH, USA; and the Ph.D. degree in civil engineering from University of California, Berkeley, CA, USA.

He is an Assistant Professor with the School of Aeronautics and Astronautics, Purdue University, West Lafayette, IN, USA. His research interests include control and optimization, with an emphasis on applications in air traffic flow management, dynamic airspace configuration and studies for the next-generation air transportation system.

AQ4

AUTHOR QUERIES

AUTHOR PLEASE ANSWER ALL QUERIES

AQ1 = Please provide keywords.

AQ2 = Please check if changes made in the affiliation note of author Gregoire Spiers are appropriate, with reference to the given biography. Please also check accuracy of postal code and location.

AQ3 = Please provide page range in Ref. [20].

AQ4 = Please check accuracy of provided location.

END OF ALL QUERIES

IEEE
Proof